Speed of Sound Measurements and Fundamental Equations of State for Octamethyltrisiloxane and Decamethyltetrasiloxane

Monika Thol[1*], Frithjof H. Dubberke[2], Elmar Baumhögger[2], Jadran Vrabec[2], Roland Span[1]

[1]Thermodynamics, Ruhr-Universität Bochum, Universitätsstraße 150, 44801 Bochum, Germany

[2]Thermodynamics and Energy Technology, Universität Paderborn, Warburger Straße 100, 33098 Paderborn, Germany

E-mail addresses:

m.thol@thermo.rub.de, Fax: +49 234 32 14163 (corresponding author)
frithjof.dubberke@uni-paderborn.de
elmar.baumhoegger@uni-paderborn.de
jadran.vrabec@uni-paderborn.de
roland.span@thermo.rub.de

ABSTRACT

Equations of state in terms of the Helmholtz energy are presented for octamethyltrisiloxane and decamethyltetrasiloxane. The restricted databases in the literature are augmented by speed of sound measurements, which are carried out by a pulse-echo method. The equations of state are valid in the fluid region up to approximately 600 K and 130 MPa and can be used to calculate all thermodynamic properties by combining the Helmholtz energy and its derivatives with respect to the natural variables. The accuracy of the equation is validated by comparison to experimental data and correct extrapolation behavior is ensured.

Keywords: Bethe-Zel'dovich-Thompson fluids, decamethyltetrasiloxane, equation of state, Helmholtz energy, octamethyltrisiloxane, speed of sound, thermodynamic properties

1 INTRODUCTION

The accurate description of thermodynamic properties of fluids is an important discipline in energy, process, and chemical engineering. For many applications in research and industry, these properties are mandatory for process simulation and the energetically but also economically efficient construction of plants. Nowadays, such information is provided by fundamental equations of state, whose parameters are adjusted to experimental data. Therefore, it is evident that the quality of the corresponding mathematical models is primarily dependent on the availability and the accuracy of experimental data. For the development of a reliable equation of state, at least homogeneous density data and information on the vapor-liquid equilibrium are required. Well established calculation of caloric properties requires fits to either isobaric heat capacity or speed of sound data, where the latter can usually be measured more precisely. Previous studies on siloxanes already showed that these fluids were barely investigated experimentally and, therefore, the development of equations of state is challenging.[1–4]

In recent years, siloxanes experienced growing interest as working fluids in organic Rankine cycle (ORC) processes, which are viable approaches for heat recovery and converting waste heat to mechanical work. In addition to the technical development of efficient hardware, design and performance of ORC processes rely on the selection of a suitable working fluid. Thus, for technically well-advanced ORC plants, reliable and accurate thermophysical property data on working fluids are a necessity.

Siloxanes belong to the wider class of organosilicone compounds and are classical examples of fluids that reveal a positive slope of the saturated vapor line. In particular, linear siloxanes, such as hexamethyldisiloxane (MM), octamethyltrisiloxane (MDM), or decamethyltetrasiloxane (MD_2M) as well as their mixtures, appear to be good candidates for becoming widely used working fluids in high-temperature ORC processes.[5] However, the current lack of accurate thermophysical data of siloxanes may lead to sub-optimally designed cycles. During the design and construction of ORC plants, accurate thermophysical property data are directly relevant for a variety of cycle components, such as expansion devices, heat exchangers, condensers, and pumps, whereas data uncertainty may decrease the performance of those devices tremendously.

Colonna and co-workers[3,4,6] developed equations of state in terms of the Helmholtz energy for various linear and cyclic siloxanes in 2006. Due to limited experimental data sets, they applied a generalized functional form for the residual contribution to the Helmholtz energy, which was originally developed for the description of non- and weakly polar fluids, such as hydrocarbons or fluorinated hydrocarbons.[7,8] Investigations of Thol *et al.* [1,2] showed that these equations are not well suited for accurate predictions of caloric properties, such as speed of

sound or isobaric heat capacity. Furthermore, Abbas *et al.*[9] measured in 2011 density data in the homogeneous liquid phase for pressures of up to 130 MPa, which identified issues of the available models in the high-pressure region. Therefore, new equations of state for octamethyltrisiloxane (MDM) and decamethyltetrasiloxane (MD_2M) are presented here, which are correlated to all available experimental data. For the appropriate description of caloric properties, additional speed of sound measurements were carried out by means of the pulse-echo technique.

Finally, the suitability of the siloxanes for the application in ORC processes is analyzed in terms of their possible affiliation to the class of Bethe-Zel'dovich-Thompson fluids as proposed by Colonna *et al.*[10]

2 SPEED OF SOUND MEASUREMENT

Octamethyltrisiloxane was purchased from Sigma Aldrich (CAS-No. 107-51-7) with a given purity of more than 99.9 vol. % and decamethyltetrasiloxane from Merck (CAS-No. 141-62-8) with a purity better than 99.8 vol. %. Aside from degassing with a vacuum pump, no further purification steps were applied to both fluids, cf. Table 1.

Table 1. Description of the samples used for the speed of sound measurements of octamethyltrisiloxane (MDM) and decamethyltetrasiloxane (MD_2M).

Chemical Name	Source	Initial Mole Fraction Purity	Purification Method	Final Mole Fraction Purity	Analysis Method
MDM	Sigma Aldrich	0.999	none	-	-
MD_2M	Merck	0.998	none	-	-

Speed of sound measurements were performed with the pulse-echo technique by determining the propagation time difference Δt of an acoustical wave burst, which propagates over known distances between two reflectors in the fluid sample, cf. Dubberke *et al.*[11] The experimental speed of sound is given by the ratio of propagation length and time, where diffraction and dispersion effects are taken into account.[12] The path length was calibrated to water for temperatures of 300 K to 400 K with pressures of 10 MPa to 120 MPa. Test measurements for water were accurate to within 0.05 %. During the present experimental work, we further developed our speed of sound apparatus so that the two fluids were sampled with different measurement approaches and measurement instrumentation.

Octamethyltrisiloxane

Speed of sound measurements were performed for octamethyltrisiloxane in the liquid state along six isotherms over a temperature range from 300 K to 550 K and for pressures up to 30 MPa, cf. Figure 1 (top).

For this fluid, the measurement of the propagation time difference Δt was based on the correlation method, which was also used by Ball and Trusler,[13] combined with signal enhancement by applying Fast Fourier Transformation (FFT) to the sampled echo signals.[14] The two echoes were identified and selected by an oscilloscope and uploaded to a computer. Noise suppression was applied to the echo signals by a FFT filter before the propagation time difference Δt was determined with a correlation function.[1] The pressure sensor was a Honeywell TJE with an operating range of up to 70 MPa and an absolute measurement uncertainty of 0.05 % with respect to the full scale. The temperature was measured with a Pt100 thermometer (Rössel Messtechnik, RM-type) with a given uncertainty of 20 mK.

The resulting experimental data together with the uncertainties based on the experimental setup are listed in Table 2.

Table 2. Experimental results for the speed of sound w of octamethyltrisiloxane (MDM). Δ_w denotes the combined expanded uncertainty ($k = 2$). The uncertainty contribution caused by the impurity of the fluid could not be estimated and was therefore not considered. However, impurities have a significant contribution to the experimental uncertainty, which may be higher than the uncertainties of the experimental setup.

T / K	p / MPa	w / m·s^{-1}	Δ_w / m·s^{-1} [a]	T / K	p / MPa	w / m·s^{-1}	Δ_w / m·s^{-1} [a]
299.619	0.101	911.32	0.92	400.020	9.928	704.99	0.92
299.627	0.502	914.41	0.92	400.150	19.875	796.17	0.84
299.636	0.984	918.29	0.92	399.420	29.701	873.39	0.82
299.644	1.480	922.14	0.92				
299.647	2.012	926.38	0.92	449.990	0.492	436.70	1.60
299.664	3.441	937.36	0.92	449.960	1.045	448.89	1.53
299.692	5.923	955.80	0.91	449.980	1.523	458.69	1.47
299.612	10.196	986.47	0.91	450.010	1.994	468.09	1.42
299.676	20.155	1050.26	0.92	450.050	3.497	495.73	1.30
299.709	30.179	1107.31	0.93	450.090	6.009	536.60	1.15
				450.140	9.983	591.45	1.01
349.908	0.111	742.97	0.97	450.220	20.246	701.94	0.85
349.686	0.558	748.58	0.96	449.440	23.518	734.50	0.82
349.647	1.075	754.20	0.96				
349.598	1.556	759.34	0.95	499.040	1.000	292.60	2.48
349.589	2.066	764.64	0.94	499.020	1.521	313.47	2.25
349.576	3.704	781.00	0.93	498.960	1.989	328.83	2.08
349.606	6.067	803.25	0.91	498.940	3.487	373.05	1.73
349.592	10.127	839.26	0.88	499.000	5.834	424.21	1.41
349.605	20.075	915.62	0.86	499.020	10.178	498.23	1.12
349.638	29.800	980.01	0.87	499.050	16.859	585.07	0.92
399.965	0.508	588.68	1.15	549.790	4.484	279.71	2.10
399.965	0.993	595.83	1.13	549.740	6.653	340.31	1.61
399.958	1.439	602.33	1.11	549.800	10.050	411.61	1.26
399.946	2.018	610.77	1.09	549.840	12.528	452.26	1.12
399.957	3.510	630.80	1.04	549.670	15.312	492.60	1.01

[a] Uncertainties ($k = 2$): temperature: 0.1 K, time difference: 0.004 µs, propagation length: 14 µm, pressure: 0.07MPa

Decamethyltetrasiloxane

Speed of sound measurements were performed for decamethyltetrasiloxane in liquid along seven isotherms over a temperature range from 219 K to 500 K and for pressures of up to 120 MPa, cf. Figure 1 (bottom).

In this case, Δt was determined by direct time difference measurement with a single burst approach in combination with burst design and signal processing, based on the peak-to-peak method (PPM). PPM relies on the fact that the maximum amplitudes occur at the equivalent time interval in both echoes and, therefore, Δt can be derived directly from the timing of those

maxima, cf. Dubberke *et al*.[15] Here, burst design helped to shape a distinct echo signal and FFT processing supported the readability of the echo signal by boosting its time resolution and suppressing noise with a bandpass filter. This procedure was necessary for measurements at high temperature and low pressure because the signal-to-noise ratio was decreasing while approaching the critical point. Pressure measurement was done by three pressure sensors, i.e. two type Keller PAA 33X 10 MPa and 100 MPa and one type TJE 200 MPa. The combination of those three pressure sensors was applied as a cascaded serial connection with an operating range of up to 200 MPa and an absolute maximum measurement uncertainty of 0.05 % with respect to the full scale, cf. Figure 2. Here, the measurements were limited to 120 MPa due to the sealing of the pressure vessel. The pressure sensor type Keller 10 MPa was calibrated with a pneumatic deadweight tester (DH-Budenberg, D&H 5200) with nitrogen. Calibration of the sensor type Keller 100 MPa was done against a hydraulic deadweight tester (DH-Budenberg, 580 EHX). Since the zero drift of sensor type TJE 200 MPa had the largest uncertainty impact, it was continuously calibrated against the 100 MPa sensor.

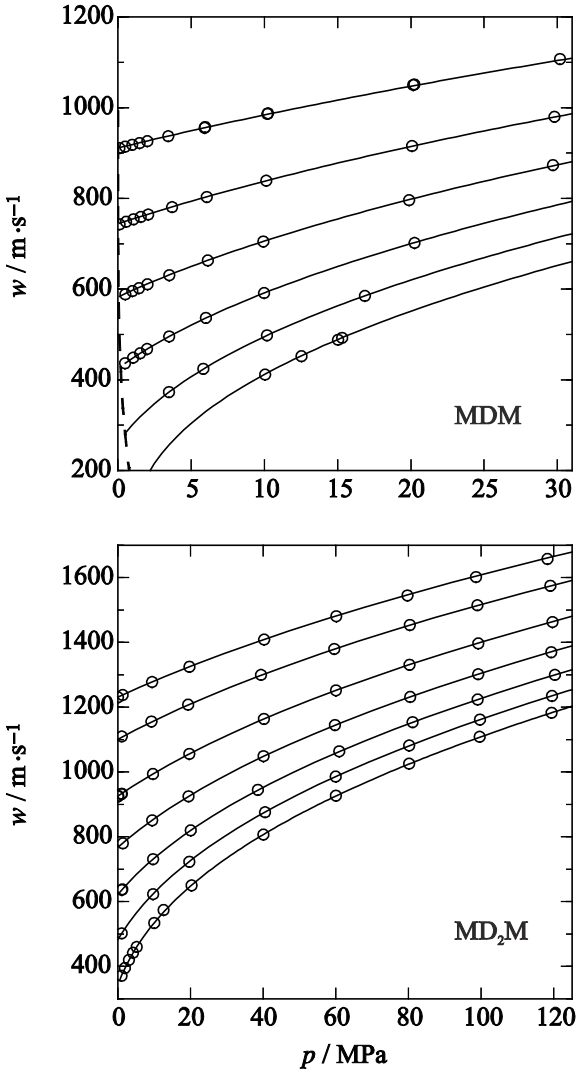

Figure 1. Speed of sound measurements of octamethyltrisiloxane (MDM) and decamethyltetrasiloxane (MD_2M). Present experimental data are depicted as circles, whereas the present equations of state are illustrated as solid curves. The dashed line, only visible for MDM, shows the speed of sound of the saturated liquid.

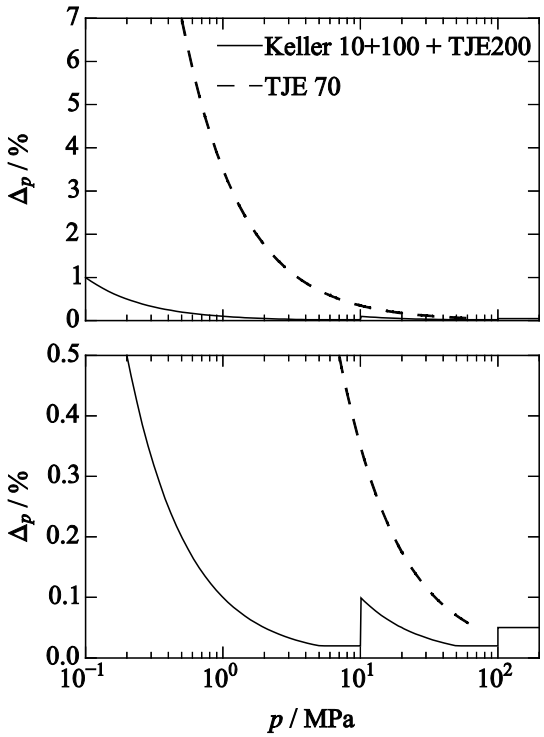

Figure 2. Uncertainty of pressure measurement Δ_p for the cascaded serial connection (CSC) of three sensors (solid line) over a pressure range from 0.1 to 200 MPa and for the TJE in a pressure range from 0.1 to 70 MPa. Below 10 MPa, the CSC presents a significantly lower pressure uncertainty compared to the single TJE sensor. The bottom plot shows a magnified view on the top plot.

The temperature was measured with a standardized 25 Ω platinum thermometer (Rosemount 162 CE, calibrated by PTB) together with a MKT 25 measuring bridge with a given overall uncertainty of 2.7 mK (regularly checked against the triple point of water). With respect to possible temperature differences between fluid and sensor position, the uncertainty of temperature measurement was estimated to 0.02 K.

The measurement range was limited for MDM (MD_2M) down to a pressure of about 4 MPa (1 MPa) along the 550 K (500 K) isotherm due to the limitation of the pulse-echo method for near critical states as a result of absorption and attenuation effects.[11]

Including the uncertainties from referencing the propagation lengths and the measurement procedure according to the error propagation law, the maximum uncertainty was about 0.8 % for MDM and 0.08 % for MD_2M ($k = 2$) with respect to the speed of sound. The uncertainty contribution caused by the impurity of the fluids could not be estimated and was therefore not considered. However, the impurities have a significant contribution to the experimental uncertainty, which is higher than the uncertainties of the experimental setup. The resulting experimental data together with the uncertainties based on the experimental setup are listed in Table 3.

Table 3. Experimental results for the speed of sound w of decamethyltetrasiloxane (MD_2M). Δ_w denotes the combined expanded uncertainty ($k = 2$). The uncertainty contribution caused by the impurity of the fluid could not be estimated and was therefore not considered. However, impurities have a significant contribution to the experimental uncertainty, which may be higher than the uncertainties of the experimental setup.

T / K	p / MPa	w / m·s^{-1}	Δ_p / MPa	Δ_w / m·s^{-1} [a]
217.814	0.002	1231.95	0.002	0.93
217.806	1.324	1238.80	0.002	0.94
217.848	9.419	1278.37	0.004	0.97
217.899	19.699	1325.19	0.020	1.01
217.992	40.255	1409.21	0.020	1.08
218.013	60.115	1481.33	0.024	1.14
218.085	79.712	1545.87	0.032	1.20
218.165	98.572	1602.99	0.039	1.25
218.238	118.233	1658.39	0.118	1.34
249.842	1.077	1110.11	0.002	0.83
249.843	9.240	1156.24	0.004	0.87
249.804	19.343	1208.71	0.020	0.91
249.800	39.384	1300.35	0.020	0.99
249.737	59.554	1380.75	0.024	1.05
249.647	80.370	1454.87	0.032	1.12
249.534	98.950	1515.20	0.040	1.17
249.424	119.047	1575.46	0.119	1.27
299.902	0.016	925.67	0.002	0.68
299.935	0.121	926.31	0.002	0.69
299.960	0.958	932.76	0.002	0.69
299.915	1.080	933.63	0.002	0.69
299.983	9.659	994.25	0.004	0.74
299.995	19.671	1056.26	0.020	0.79
300.006	40.202	1164.31	0.020	0.87
300.002	60.024	1252.37	0.024	0.94
300.005	80.266	1331.24	0.032	1.01
300.004	99.198	1397.65	0.040	1.07
300.035	119.626	1463.06	0.120	1.18
349.925	1.369	780.56	0.002	0.57
349.890	9.447	851.51	0.004	0.62
349.899	19.447	925.37	0.020	0.69
349.928	40.092	1049.16	0.020	0.78
349.867	59.744	1145.45	0.024	0.86
349.918	80.462	1232.54	0.032	0.93
349.895	99.170	1302.54	0.040	0.99
349.892	119.296	1370.82	0.119	1.11
399.597	1.077	636.31	0.002	0.47
399.665	1.234	638.18	0.002	0.47
399.596	9.691	731.33	0.004	0.53
399.669	20.055	820.52	0.020	0.62
399.685	38.533	945.04	0.020	0.70
399.695	60.934	1064.32	0.024	0.79
399.696	81.120	1154.26	0.032	0.86
399.696	99.014	1224.64	0.040	0.92

399.553	120.290	1300.12	0.120	1.06
450.052	1.060	502.02	0.002	0.37
449.895	9.702	623.33	0.004	0.45
449.920	19.667	723.35	0.020	0.55
449.959	40.506	876.94	0.020	0.65
449.990	59.941	986.94	0.024	0.73
450.013	80.184	1082.55	0.032	0.81
450.029	99.670	1162.66	0.040	0.87
450.039	119.488	1235.39	0.119	1.01
499.757	1.001	371.60	0.002	0.29
499.824	1.926	395.00	0.002	0.30
499.777	3.058	420.07	0.002	0.31
499.717	4.164	442.17	0.002	0.32
499.749	5.168	460.32	0.002	0.34
499.608	9.979	534.61	0.004	0.39
499.669	20.291	650.54	0.020	0.50
499.695	40.057	807.98	0.020	0.60
499.722	60.022	927.39	0.024	0.68
499.751	80.169	1026.54	0.032	0.76
499.802	99.589	1109.02	0.040	0.83
499.886	119.374	1183.60	0.119	0.98

[a] Expanded uncertainties ($k = 2$): temperature: 0.04 K, time difference: 0.004 µs, propagation length: 14 µm

3 EQUATIONS OF STATE

The present equations of state are expressed in terms of the Helmholtz energy a, which is reduced by the universal gas constant (R = 8.3144598 J·mol^{-1}·K^{-1} according to the 2014 CODATA recommendations[16]) and the temperature T

$$\alpha(\tau,\delta) = \frac{a(T,\rho)}{RT}. \tag{1}$$

Furthermore, the reduced Helmholtz energy α is separated into an ideal (superscript ^{o}) and a residual contribution (superscript ^{r}). The ideal part describes the effects of density independent intramolecular energy of the hypothetical ideal gas state, whereas the residual part considers the intermolecular interactions and possible effects of density dependent intramolecular interactions

$$\alpha(\tau,\delta) = \alpha^{o}(\tau,\delta) + \alpha^{r}(\tau,\delta). \tag{2}$$

Due to practical reasons, the natural variables temperature and density are reduced by the critical parameters of the investigated fluid

$$\tau = \frac{T_c}{T} \quad \text{and} \quad \delta = \frac{\rho}{\rho_c}. \tag{3}$$

For the isobaric heat capacity of the ideal gas, a simplified rigid rotator, harmonic oscillator approach according to Span[17] was applied

$$\frac{c_p^{o}}{R} = (c_0 + 1) + \sum_{i=1}^{I_{Pol}} n_i^{*} T^{t_i^{*}} + \sum_{k=1}^{K_{PE}} m_k \left(\frac{\theta_k}{T}\right)^2 \frac{\exp(\theta_k/T)}{\left(\exp(\theta_k/T)-1\right)^2}. \tag{4}$$

Due to the relation between the reduced Helmholtz energy and the isochoric heat capacity

$$\left(\frac{\partial^2 \alpha^{o}}{\partial \tau^2}\right)_{\delta} = -\frac{c_v^{o}}{R\tau^2}, \quad \text{with} \quad c_v^{o} = c_p^{o} - R \tag{5}$$

a two-fold integration yields the ideal gas contribution to the residual Helmholtz energy

$$\alpha^{o}(\tau,\delta) = c^{II} + c^{I}\tau + c_0 \ln(\tau) + \sum_{i=1}^{I_{Pol}} c_i \tau^{t_i} + \sum_{k=1}^{K_{PE}} m_k \ln\left[1 - \exp\left(-\theta_k/T_c\,\tau\right)\right] + \ln(\delta), \tag{6}$$

with $c_i = -n_i^{*} \Big/ \left(t_i^{*}\left(t_i^{*}+1\right)\right) T_c^{t_i^{*}}$ and $t_i = -t_i^{*}$.

In this work, only Planck-Einstein terms were used. The corresponding parameters are listed in Table 4.

The integration constants c^{I} and c^{II} can be chosen arbitrarily. Here, the normal boiling point reference state was applied, which is common practice in the literature for many fluids. Thus, the constants are calculated such that enthalpy and entropy are zero at the boiling temperature T_B(p = 0.101325 MPa) and the corresponding saturated liquid density ρ'(p = 0.101325 MPa).

Table 4. Parameters of the ideal part of the present equations of state, cf. Eq (6).

i	1	2	3	c_0	c^{I}	c^{II}
Octamethyltrisiloxane (MDM)						
m_i	28.817	46.951	31.054	3	−19.6600754	117.994606
θ_i / K	20	1570	4700			
Decamethyltetrasiloxane (MD_2M)						
m_i	28.59	56.42	50.12	3	−26.3839138	131.089725
θ_i / K	20	1180	4240			

The residual contribution to the reduced Helmholtz energy consists of three empirical term types:

$$\begin{aligned}\alpha^{\mathrm{r}}(\tau,\delta) &= \alpha^{\mathrm{r}}_{\mathrm{Pol}}(\tau,\delta)+\alpha^{\mathrm{r}}_{\mathrm{Exp}}(\tau,\delta)+\alpha^{\mathrm{r}}_{\mathrm{GBS}}(\tau,\delta)\\ &= \sum_{i=1}^{I_{\mathrm{Pol}}} n_i\delta^{d_i}\tau^{t_i} + \sum_{i=I_{\mathrm{Pol}}+1}^{I_{\mathrm{Pol}}+I_{\mathrm{Exp}}} n_i\delta^{d_i}\tau^{t_i}\exp\left(-\delta^{p_i}\right)\\ &+ \sum_{i=I_{\mathrm{Pol}}+I_{\mathrm{Exp}}+1}^{I_{\mathrm{Pol}}+I_{\mathrm{Exp}}+I_{\mathrm{GBS}}} n_i\delta^{d_i}\tau^{t_i}\exp\left(-\eta_i\left(\delta-\varepsilon_i\right)^2-\beta_i\left(\tau-\gamma_i\right)^2\right).\end{aligned} \tag{7}$$

In principle, polynomial ($_{\mathrm{Pol}}$) and exponential ($_{\mathrm{Exp}}$) terms are sufficient for an accurate description of thermodynamic properties in the entire fluid region. However, the introduction of modified Gaussian bell-shaped terms ($_{\mathrm{GBS}}$) by Setzmann and Wagner[18] enables a better representation of the critical region. Nowadays, these terms are also used in other regions with moderate parameters, which results in a smaller overall number of terms.

Table 5. Parameters of the residual part of the present equation of state for octamethyltrisiloxane (MDM), cf. Eq. (7).

i	n_i	t_i	d_i	p_i	η_i	β_i	γ_i	ε_i
1	$5.039724\cdot10^{-2}$	1.000	4	-				
2	$1.189992\cdot10^{+0}$	0.188	1	-				
3	$-2.468723\cdot10^{+0}$	1.030	1	-				
4	$-7.438560\cdot10^{-1}$	0.700	2	-				
5	$4.434056\cdot10^{-1}$	0.464	3	-				
6	$-1.371359\cdot10^{+0}$	2.105	1	2				
7	$-1.529621\cdot10^{+0}$	1.376	3	2				
8	$4.445898\cdot10^{-1}$	0.800	2	1				
9	$-1.009921\cdot10^{+0}$	1.800	2	2				
10	$-5.903694\cdot10^{-2}$	1.005	7	1				
11	$3.515188\cdot10^{+0}$	0.700	1	-	0.986	0.966	1.250	0.928
12	$8.367608\cdot10^{-2}$	0.660	1	-	1.715	0.237	1.438	2.081
13	$1.646856\cdot10^{+0}$	1.138	3	-	0.837	0.954	0.894	0.282
14	$-2.851917\cdot10^{-1}$	1.560	2	-	1.312	0.861	0.900	1.496
15	$-2.457571\cdot10^{+0}$	1.310	2	-	1.191	0.909	0.899	0.805

Table 6. Parameters of the residual part of the present equation of state for decamethyltetrasiloxane (MD_2M), cf. Eq. (7).

i	n_i	t_i	d_i	p_i	η_i	β_i	γ_i	ε_i
1	$1.458333\cdot10^{-2}$	1.000	4	-				
2	$3.227554\cdot10^{+0}$	0.319	1	-				
3	$-3.503565\cdot10^{+0}$	0.829	1	-				
4	$-2.017391\cdot10^{+0}$	0.780	2	-				
5	$8.606129\cdot10^{-1}$	0.687	3	-				
6	$-2.196015\cdot10^{+0}$	1.290	1	2				
7	$-9.289014\cdot10^{-1}$	3.910	3	2				
8	$2.027740\cdot10^{+0}$	0.770	2	1				
9	$-9.168439\cdot10^{-1}$	3.055	2	2				
10	$-6.383507\cdot10^{-2}$	1.013	7	1				
11	$2.674255\cdot10^{+0}$	1.070	1	-	0.982	0.7323	1.0420	0.874
12	$4.662529\cdot10^{-2}$	1.890	1	-	2.700	0.5430	1.1000	1.430
13	$-3.835361\cdot10^{-1}$	1.133	3	-	1.347	1.2600	1.1460	0.855
14	$-4.273462\cdot10^{-1}$	0.826	2	-	0.864	0.8780	1.0850	0.815
15	$-1.148009\cdot10^{+0}$	0.830	2	-	1.149	2.2200	0.6844	0.491

In this work, a non-linear fitting algorithm provided by the National Institute of Standards and Technology[19] was applied to determine the fluid-specific parameters. The basic features of the fitting algorithm were described by Lemmon and Jacobsen.[20] Since a non-linear fitting technique requires adequate initial parameter values, it is beneficial to start the fitting procedure with a functional form of another fluid, which is known to yield physically reasonable results and exhibits correct extrapolation behavior. Here, the equation of state for chlorine[21] was applied. From this starting point, all parameters were optimized, including coefficients, temperature and density exponents, Gaussian bell-shaped parameters, and the number of terms. The resulting parameters for octamethyltrisiloxane and decamethyltetrasiloxane are given in Tables 5 and 6. For both fluids, five polynomial, five exponential, and five Gaussian bell-shaped terms were chosen.

Form this equation, all thermodynamic properties in the homogeneous state region can be calculated by means of the reduced Helmholtz energy and its derivatives with respect to the natural variables, see Span[17] or Lemmon *et al.*[22] For the calculation of vapor pressure and saturated densities, an iterative procedure taking into account the thermal, mechanic, and chemical equilibrium has to be applied. For computer calculations, it is helpful to use ancillary equations to generate initial values for these iterations. Therefore, ancillary equations for vapor pressure, saturated liquid density, and saturated vapor density were developed, see Eqs. (8) to (10). The parameters are given in Table 7. These ancillary equations are no reference equations so that the fundamental equations of state must be used to calculate accurate saturation properties.

Vapor pressure $$\ln\left(\frac{p_{\mathrm{v}}}{p_{\mathrm{c}}}\right)=\left(\frac{T_{\mathrm{c}}}{T}\right)\sum_{i=1}^{5}n_i\left(1-\frac{T}{T_{\mathrm{c}}}\right)^{t_i} \quad (8)$$

Saturated liquid density $$\frac{\rho'}{\rho_{\mathrm{c}}}=1+\sum_{i=1}^{5}n_i\left(1-\frac{T}{T_{\mathrm{c}}}\right)^{t_i} \quad (9)$$

Saturated vapor density $$\ln\left(\frac{\rho''}{\rho_{\mathrm{c}}}\right)=\sum_{i=1}^{6}n_i\left(1-\frac{T}{T_{\mathrm{c}}}\right)^{t_i} \quad (10)$$

Table 7. Parameters for the ancillary equations of octamethyltrisiloxane (MDM) and decamethyltetrasiloxane (MD_2M).

	p_v: Eq. (8)		ρ': Eq. (9)		ρ'': Eq. (10)	
			Octamethyltrisiloxane (MDM)			
i	n_i	t_i	n_i	t_i	n_i	t_i
1	−8.8192	1.00	7.016	0.54	−5.3686	0.515
2	4.0952	1.50	−13.924	0.90	−11.85	4.580
3	−4.062	1.90	20.84	1.30	−16.64	2.060
4	−6.208	3.71	−16.64	1.73	−52.26	5.250
5	−3.212	14.6	5.906	2.20	−125.6	11.30
6					−235.7	21.60
			Decamethyltetrasiloxane (MD_2M)			
1	−10.174	1.00	8.215	0.498	−4.5483	0.428
2	9.607	1.50	−24.65	0.855	−101.989	2.320
3	−10.08	1.83	47.23	1.220	224.06	2.800
4	−7.242	4.15	−42.44	1.600	−182.79	3.300
5	−30.56	17.8	15.18	2.040	−110.45	8.500
6					−330.87	17.50

4 COMPARISON TO EXPERIMENTAL DATA

In this section, the present equations of state are compared to experimental data. Figure 3 shows all experimental data in the homogeneous state. The red symbols depict data, which were available for the development of the equations of state of Colonna *et al.*[4] in 2008. For MDM at that time, there were only density data in the gaseous region and in the liquid state at atmospheric pressure available. Only a few state points in the liquid state at atmospheric pressure could be considered for the speed of sound. In the case of MD_2M in 2008, there were not even measurements in the gaseous state available. Therefore, it is not surprising that the equations of Colonna *et al.*[4] show disadvantages in the representation of homogeneous density data at elevated pressure and in the representation of caloric properties.

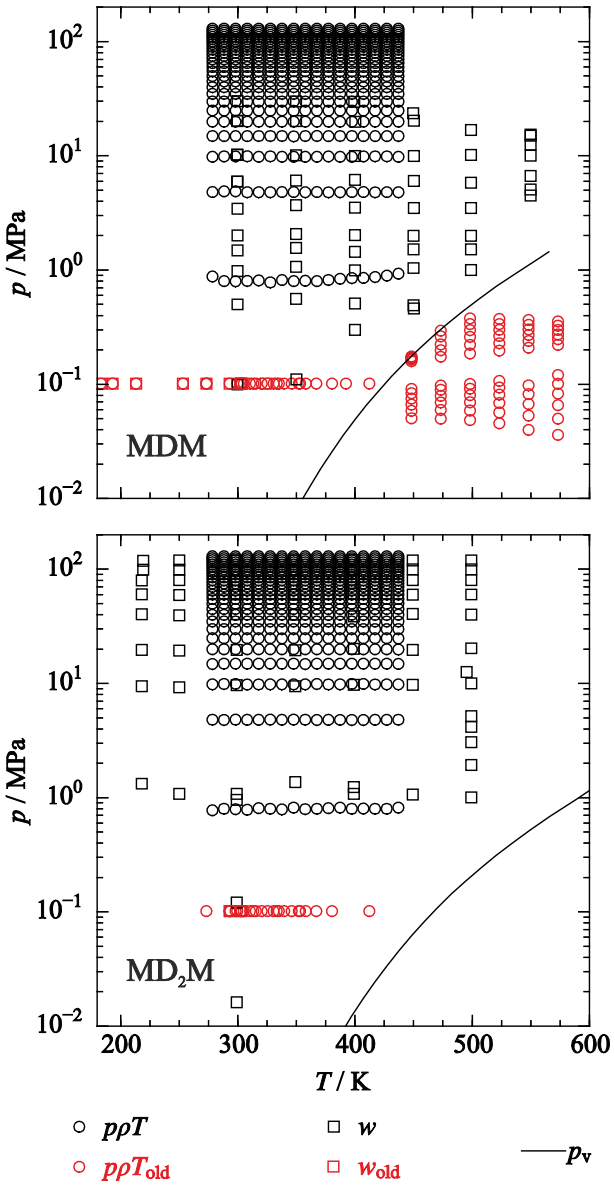

Figure 3. Available experimental data for octamethyltrisiloxane (MDM) and decamethyltetrasiloxane (MD_2M) in the homogeneous region. The red symbols depict data that were available in 2008 for the development of the equations of state of Colonna *et al.*[4].

In 2011, Abbas *et al.*[9] published comprehensive density measurements, which were considered for the development of the present equations of state. Furthermore, the present speed of sound data as described in section 2 were applied. Based on these data, the new equation for MDM is valid from the triple point temperature T_{tr} = 187.2 K to T_{max} = 570 K and a maximum pressure of 130 MPa. The equation for MD_2M is valid from the triple point temperature T_{tr} = 205.2 K according to Rowley *et al.*[23] to T_{max} = 600 K and a maximum pressure of 130 MPa. Other fluid-specific properties are given in Table 8

Table 8. Fluid-specific properties of octamethyltrisiloxane (MDM) and decamethyltetrasiloxane (MD_2M). If no reference is given, the property was calculated in this work.

	MDM	**Ref.**	**MD_2M**	**Ref.**
T_c / K	565.3609	[24]	599.4	[24]
ρ_c / mol·dm^{-3}	1.134	[25]	0.864	[26]
p_c / MPa	1.4375		1.144	
T_B / K	425.63		467.59	
T_{tr} / K	187.2	[23]	205.2	[23]
$\rho_{tr,liq.}$ / mol·dm^{-3}	3.907		3.032	
M / g·mol^{-1}	236.5315	[27]	310.6854	[27]

In the following, percentage deviations between the equations of state and experimental data were calculated according to

$$\Delta X = 100 \frac{X_{\mathrm{DATA}} - X_{\mathrm{EOS}}}{X_{\mathrm{DATA}}}. \tag{11}$$

To quantify the representation of the experimental data, the average absolute relative deviation was evaluated for each author according to

$$\mathrm{AAD} = \frac{1}{N} \sum_{i=1}^{N} \left| \Delta X_i \right|. \tag{12}$$

Vapor-liquid equilibrium data are classified in three different temperature ranges in relation to the critical temperature.

Table 9. Average absolute relative deviations of experimental vapor pressure, saturated liquid, and saturated vapor density data from the present equation of state for octamethyltrisiloxane (MDM). Temperatures were adapted to the ITS-90 scale.

	No. of	Temperature	AAD / %			
Author	**points**	**range / K**	**LT**	**MT**	**HT**	**overall**
Vapor pressure						
Abbas *et al.*[9]	23	292 - 426	3.29	3.87	-	3.64
Flaningam[26]	12	346 - 437	-	0.075	-	0.075
Lindley & Hershey[25]	74	322 - 565	2.80	0.42	0.27	0.45
Patnode & Wilcock[28]	1	426.14	-	1.33	-	1.33
Reuther & Reichel[29]	7	273 - 344	5.21	0.98	-	4.60
Thompson[30]	1	426.14	-	0.50	-	0.50
Wilcock[31]	10	280 - 424	11.2	5.74	-	7.96
Saturated liquid density						
Lindley & Hershey[25]	34	273 - 564	0.13	0.27	1.02	0.40
Saturated vapor density						
Lindley & Hershey[25]	18	460 - 565	-	0.45	1.22	0.75

[a] LT: $T/T_c < 0.6$; MT: $0.6 \leq T/T_c \leq 0.98$; HT: $T/T_c > 0.98$

Table 10. Average absolute relative deviations of the experimental data of homogeneous states from the present equation of state octamethyltrisiloxane (MDM). Temperatures were adapted to the ITS-90 scale.

	No. of	Temperature	Pressure	AAD / %
Author	**points**	**range / K**	**range / MPa**	
Isobaric heat capacity of the ideal gas				
Nannan & Colonna[32]	10	298 - 1201	$p \rightarrow 0$	0.17
Density				
Abbas *et al.*[9]	459	278 - 438	0.8 - 130	0.044
Golik & Cholpan[33]	1	303.13	0.101325	0.23
Hurd[34]	5	273 - 354	0.101325	0.089
Marcos *et al.*[35]	70	448 - 574	<0.1 - 1	0.51
McLure *et al.*[36]	17	299 - 413	0.101325	0.065
Sperkach & Cholpan[37]	6	183 - 304	0.101325	0.17
Speed of sound				
This work	*48*	*299 - 550*	*0.1 - 31*	*0.10*
Golik & Cholpan[33]	1	303.13	0.101325	0.11
Sperkach & Choplan[37]	6	183 - 304	0.101325	1.91
Waterman *et al.*[38]	1	293.14	0.101325	2.63
Weissler[39]	2	303 - 324	0.101325	0.17
Isobaric heat capacity				
Abbas *et al.*[9]	38	213 - 394	p_v	0.21
McLure & Neville[40]	2	303 - 324	p_v	1.95

Author	No. of points	Temperature range / K	Pressure range / MPa	AAD / %
Heat of vaporization				
Wabiszczewicz[41]	33	294 - 401	p_v	2.08
Second virial coefficient (AAD in cm³·mol⁻¹)				
Marcos *et al.*[35]	6	448 - 574	$p \rightarrow 0$	32.4

Table 11. Average absolute relative deviations of experimental vapor pressure data from the present equation of state for decamethyltetrasiloxane (MD_2M). Temperatures were adapted to the ITS-90 scale.

Author	No. of points	Temperature range / K	AAD / % LT	MT	HT	overall
Abbas *et al.*[9]	23	320 - 468	4.56	3.74	-	3.95
Flaningam[26]	15	366 - 480	-	0.066	-	0.066
Hurd [34]	1	467.00	-	1.42	-	1.42
Waterman *et al.* [38]	1	467.65	-	0.15	-	0.15
Wilcock [31]	2	361 - 468	-	0.96	-	0.96

Table 12. Average absolute relative deviations of the experimental data of homogeneous states from the present equation of state for decamethyltetrasiloxane (MD_2M). Temperatures were adapted to the ITS-90 scale.

Author	No. of points	Temperature range / K	Pressure range / MPa	AAD / %
Isobaric heat capacity of the ideal gas				
Nannan & Colonna[32]	11	298 - 1401	$p \rightarrow 0$	1.55
Density				
Abbas *et al.*[9]	459	278 - 438	0.8 - 130	0.05
Fox *et al.*[42]	1	293.14	0.101325	0.25
Golik & Cholpan[33]	1	303.13	0.101325	0.058
Hunter *et al.*[43]	1	298.14	0.101325	0.33
Hurd[34]	5	273 - 354	0.101325	0.034
Matteoli *et al.*[44]	1	303.15	0.101325	0.53
McLure *et al.*[36]	16	299 - 413	0.101325	0.12
Povey *et al.*[45]	1	293.15	0.101325	0.03
Waterman *et al.*[38]	1	293.14	0.101458	0.05
Speed of sound				
This work	*66*	*218 - 500*	*0.0 - 121*	*0.057*
Golik & Cholpan[33]	1	303.13	0.101325	0.55
Povey *et al.*[45]	1	293.15	0.101325	0.61
Waterman *et al.*[38]	1	293.14	0.101325	0.40
Isobaric heat capacity				
Abbas *et al.*[9]	45	228 - 439	p_v	0.40

Author	No. of points	Temperature range / K	Pressure range / MPa	AAD / %
Heat of vaporization				
Hurd[34]	1	467.00	p_v	0.85
Matteoli *et al.*[44]	1	298.15	p_v	5.25
Wilcock[31]	1	467.51	p_v	16.2

4.1 Ideal Gas State

The ideal contribution to the reduced Helmholtz energy was calculated by means of a two-fold integration of the isobaric heat capacity of the ideal gas with respect to the temperature, cf. section 3. For simplification, it was assumed that translation and rotation are always excited and molecules behave like rigid rotators and harmonic oscillators, cf. Span.[17] Hence, for complex molecules, such as siloxanes, $c_p^\circ / R = 4$ for $T \to 0$ K holds. Furthermore, m_i and θ_i of Eqs. (4) and (6) were treated as adjustable parameters.[17] For both siloxanes, three temperature dependent terms were sufficient to represent the available data with a reasonable accuracy.

For the adjustment of these parameters, there was only one data set of Nannan and Colonna[32] available. These data were predicted by means of *ab initio* calculations and an uncertainty of 6 % was reported. Figure 4 shows the representation of these data with the present equations of state. For octamethyltrisiloxane, the data can be reproduced within 0.5 %, whereas the equation of decamethyltetrasiloxane shows deviations of up to 3.2 %. Although both deviations are clearly within the specified uncertainty, the significant quality difference between both equations was further investigated. The publication of Nannan and Colonna[32] contains data for six linear and six cyclic siloxanes. c_p° data are not available for comparison with none of the others, except for hexamethyldisiloxane (MM). The representation of the hexamethyldisiloxane data is illustrated in Figure 5. Accurate measurements were presented up to 500 K and calculated for higher temperatures by Scott *et al.*[46] Their uncertainty was claimed to be 0.1 %, which could be confirmed with a recent equation of state.[1] However, the data of Nannan and Colonna[32] deviate from the data of Scott *et al.*[46] and the equation of state by up to 3 %. Especially in the low-temperature region, deviations increase. This is in line with the representation of the c_p° data of decamethyltetrasiloxane. Similar to hexamethyldisiloxane, deviations increase with decreasing temperature and reach up to approximately 3 %. A better representation of these data could not be achieved without compromising the speed of sound and isobaric heat capacity data from experiments. Therefore, it is assumed that the representation of the decamethyltetrasiloxane data is reasonable.

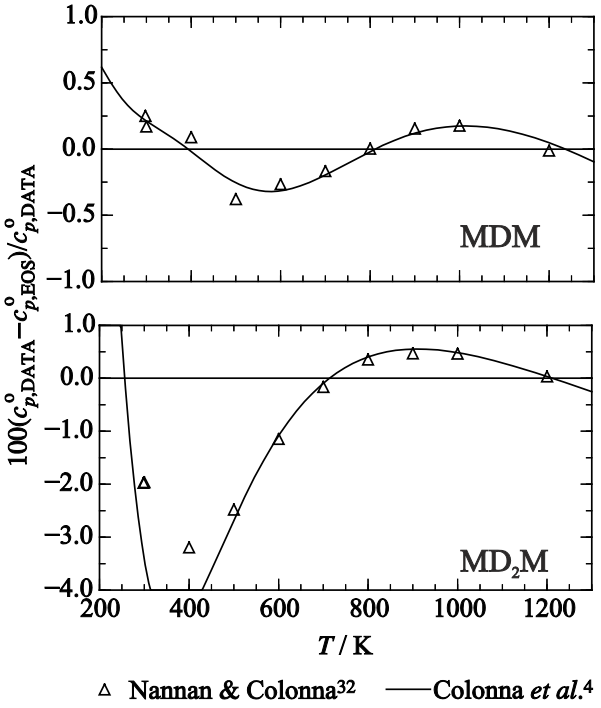

Figure 4. Representation of the isobaric heat capacity of the ideal gas of octamethyltrisiloxane (MDM) and decamethyltetrasiloxane (MD_2M) with the present equations of state.

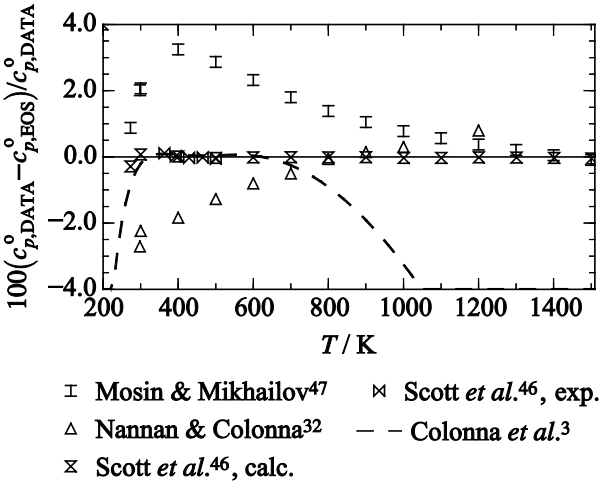

Figure 5. Representation of the isobaric heat capacity data of the ideal gas for hexamethyldisiloxane (MM) with the equation of state of Thol *et al.* [1]

4.2 Thermal properties

Figure 6 shows the representation of the vapor pressure data for both fluids. For octamethyltrisiloxane, there are measurements available between 273 K and 565 K. Some of these data were already available for hexamethyldisiloxane and octamethylcyclotetrasiloxane (D_4) as investigated in detail by Thol *et al.*[1,2] Similar to MM and D_4, the vapor pressure data of Abbas *et al.*[9] exhibit a systematic negative offset of approximately 4 % and increasing deviations for decreasing temperatures. As discussed before,[1] this behavior is most likely caused by an erroneous handling of the comparative ebulliometer. Therefore, these data were not considered for the development of the present equations of state. The data of Flaningam[26]

are represented within 0.15 %. In this publication,[26] the author does not give any information about experimental uncertainties. However, when comparing to the equation of state and other experimental measurements for hexamethyldisiloxane and octamethylcyclotetrasiloxane, an uncertainty of approximately 0.5 % can be assumed. For temperatures $T > 437$ K, only one data set published by Lindley and Hershey[25] is available. During their measurements,[25] they applied two different measurement devices. In the temperature range from 322 K to 426 K, a Swietoslawski ebulliometer was utilized. They state their temperature measurement to be accurate within 0.1 K and their pressure measurements within 3.4 kPa to 7 kPa. When considering the lower value of 3.4 kPa, the uncertainty of the vapor pressure measurements is already above 3 % in the best case. However, except for some outliers, the data scatter around the present equation of state within 0.5 % and the data of Flaningam.[26] Therefore, the specified uncertainties seem to be too large and the data were used for the fit.

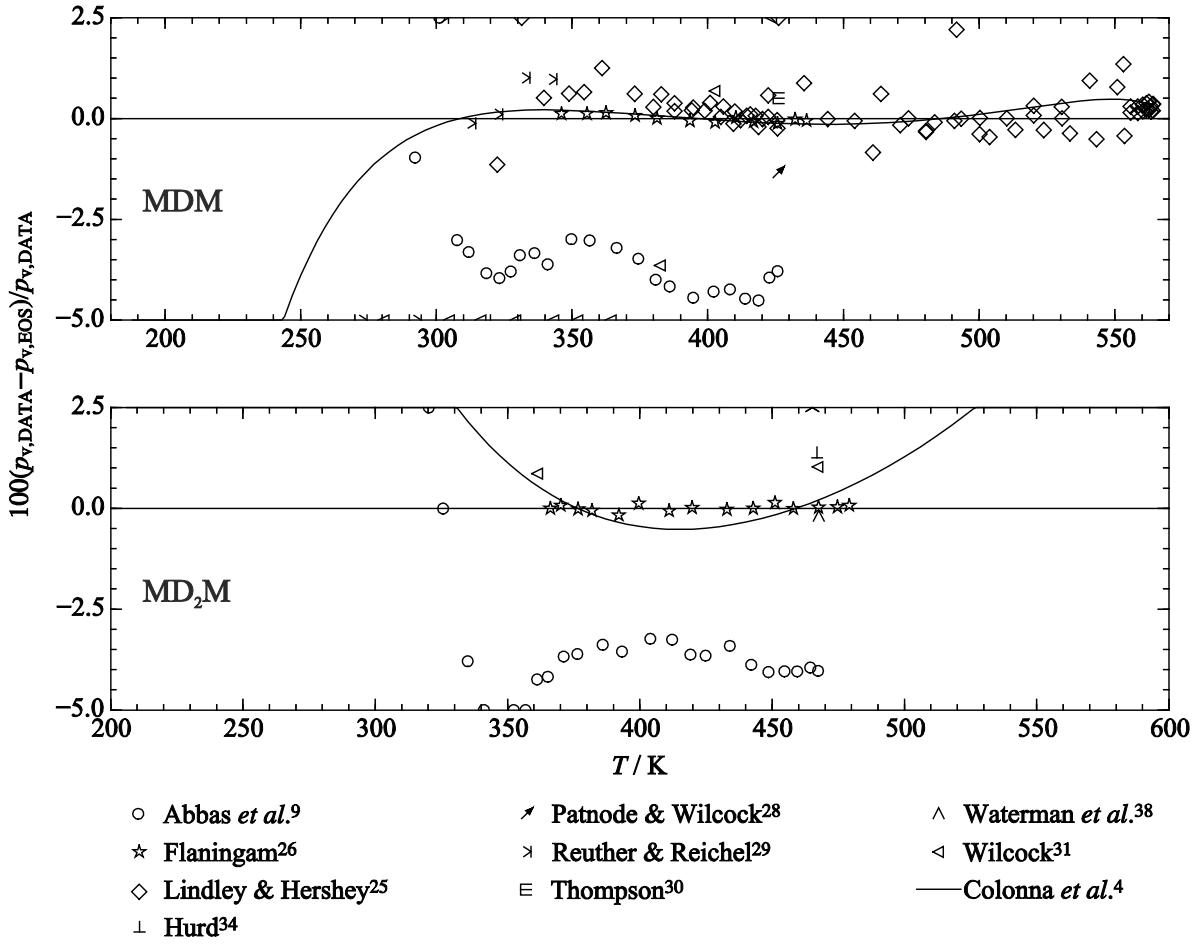

Figure 6. Relative deviations of the vapor pressure data for octamethyltrisiloxane (MDM) and decamethyltetrasiloxane (MD_2M) from the present equations of state.

The high temperature range ($T > 426$ K) was investigated by means of a Kay type $p\rho T$ apparatus.[48,49] Since it was originally designed to determine saturated vapor and liquid densities, the accuracy of the vapor pressure measurements is slightly lower than what can be achieved with an ebulliometer. However, these data can be reproduced within the same accuracy as the

low temperature data. Based on the data of Flaningam[26] and Lindley and Hershey[25], the accuracy of vapor pressure data calculated with the present equation of state for octamethyltrisiloxane is estimated to be 0.5 %.

For decamethyltetrasiloxane, only the two data sets of Flaningam[26] and Abbas *et al.*[9] containing more than two data points are available. As stated above, the data of Abbas *et al.*[9] were not considered here. Since the data of Flaningam[26] only cover a restricted temperature range (366 K to 480 K), a reliable estimation of the accuracy of vapor pressure data calculated with the present equation of state is not possible. However, the data are reproduced similarly to the data of octamethyltrisiloxane. Therefore, at least in this temperature range an uncertainty of 0.5 % can be assumed.

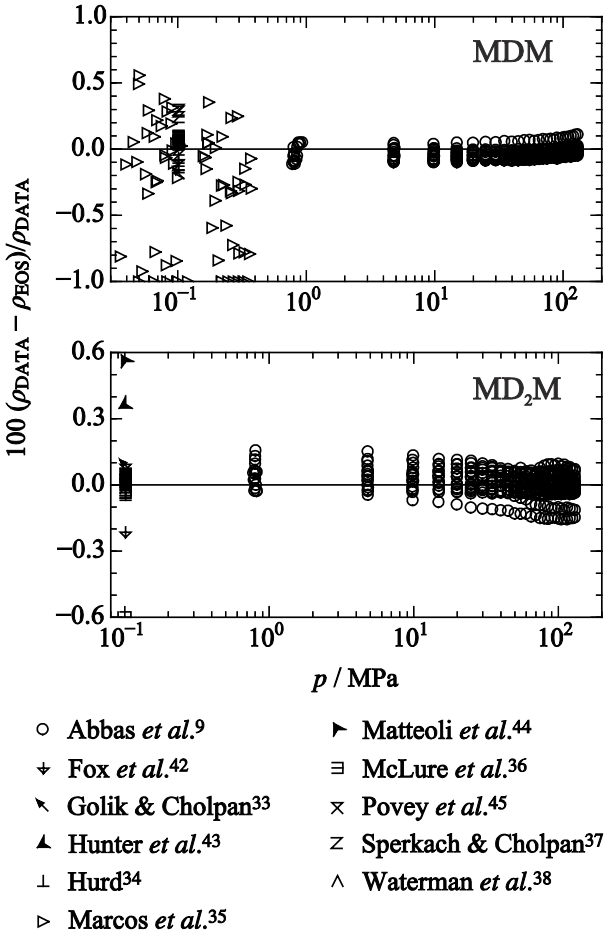

Figure 7. Relative deviations of the homogeneous density data for octamethyltrisiloxane (MDM) and decamethyltetrasiloxane (MD_2M) from the present equations of state.

In Figure 7, relative deviations of density data in homogeneous states from the present equations of state are shown. In addition to the present speed of sound measurements, density data in the liquid state published by Abbas *et al.*[9] are the most comprehensive and reliable datasets for both siloxanes. Moreover, they are the only density data at elevated pressures. For their measurement, Abbas *et al.*[9] used an Anton Paar vibrating tube densimeter, which was calibrated with water and heptane. Test measurements agreed with the corresponding equations

of state[50,51] within 0.04 % and 0.08 %. The sample purity is reported to be better than 99.8 % with a maximum water content below 100 ppm. Individual uncertainties are not clearly defined in the publication.[9] Only a temperature reproducibility (0.01 K) and an uncertainty value for the density measurement (0.1 mg·cm^{-3}) are reported. Therefore, the works of Abbas[52] and Schedemann[53] as well as results for hexamethyldisiloxane[1] were considered here for an assessment. Based on these results and the sample purity, an uncertainty of 0.1 % to 0.15 % is assumed for both fluids. Figure 7 shows that the new equations of state reproduce these data within the assumed uncertainty. For octamethyltrisiloxane, only five data points out of 459 exhibit a deviation above 0.1 % (maximum deviation: 0.11 %) from the present equation of state. For decamethyltetrasiloxane, the highest isotherm (T = 437 K) is represented with deviations between 0.1 % and 0.15 %. Among the remaining 432 state points, only 23 data points deviate by more than 0.1 % (maximum deviation: 0.15 %). Therefore, the uncertainty of density of the homogeneous liquid state calculated with the present equations of state is estimated to be within 0.15 %.

Moreover, these data are not only important for the correct behavior of the equations of state at elevated pressures. Because of the restricted data situation, they were also applied to adjust the saturated liquid density.

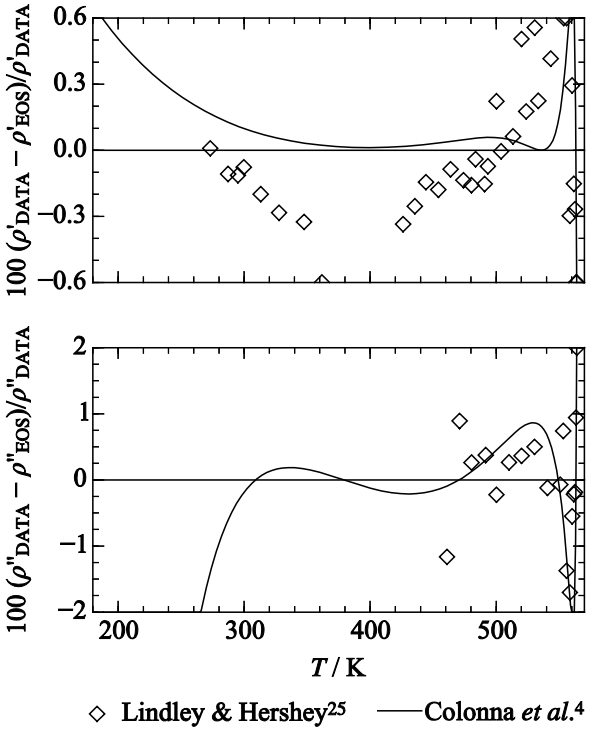

Figure 8. Relative deviations of the saturated liquid (top) and vapor (bottom) density data from the present equation of state for octamethyltrisiloxane (MDM).

In Figure 8, relative deviations of the saturated liquid and vapor density data from the present equation of state for octamethyltrisiloxane are illustrated. The measurements of Lindley and Hershey[25] are the only data available in the literature and cover a restricted temperature

range. Since the homogeneous density data of Abbas *et al.*[9] are located sufficiently close to the saturated liquid line, the vapor-liquid equilibrium was mainly controlled by these data and the vapor pressure data. To ensure low uncertainties of the saturation densities over the entire temperature range, a linear rectilinear diameter according to $\rho_{RD} = (\rho' + \rho'')/2$ was applied as a constraint to the fit, which ends at the critical point given in Table 8. In this way, not only the saturated liquid but also the saturated vapor line could be modeled in least qualitatively correctly. In the case of octamethyltrisiloxane, the saturated densities of Lindley and Hershey [25] were employed to verify this approach, which was already successfully adopted for the development of the equation of state for hexamethyldisiloxane.[1] The information on the uncertainties given in the publication of Lindley and Hershey [25] is not sufficient to estimate a combined uncertainty of their density measurements; no statement on the accuracy of the present equation with respect to the saturated densities can be made. However, the saturated liquid density data are reproduced within 0.5 %, whereas the saturated vapor density data are represented within 1.5 %. Considering the measurement technique and the sample purity of 99 %, these deviations are reasonable. For the saturated densities of decamethyltetrasiloxane, no experimental data are available in the literature to verify the phase boundaries.

Due to the limited database, a linear rectilinear diameter was applied in the critical region and the critical point reported in Table 8 was applied to the fit. A correct behavior of the isotherms in this region was controlled by modeling a saddle point of the critical isotherm at the critical point for both fluids (cf. Figure 9):

$$\left(\frac{\partial p}{\partial \rho}\right)_{T_c} = 0 \quad \text{and} \quad \left(\frac{\partial^2 p}{\partial \rho^2}\right)_{T_c} = 0\,. \tag{13}$$

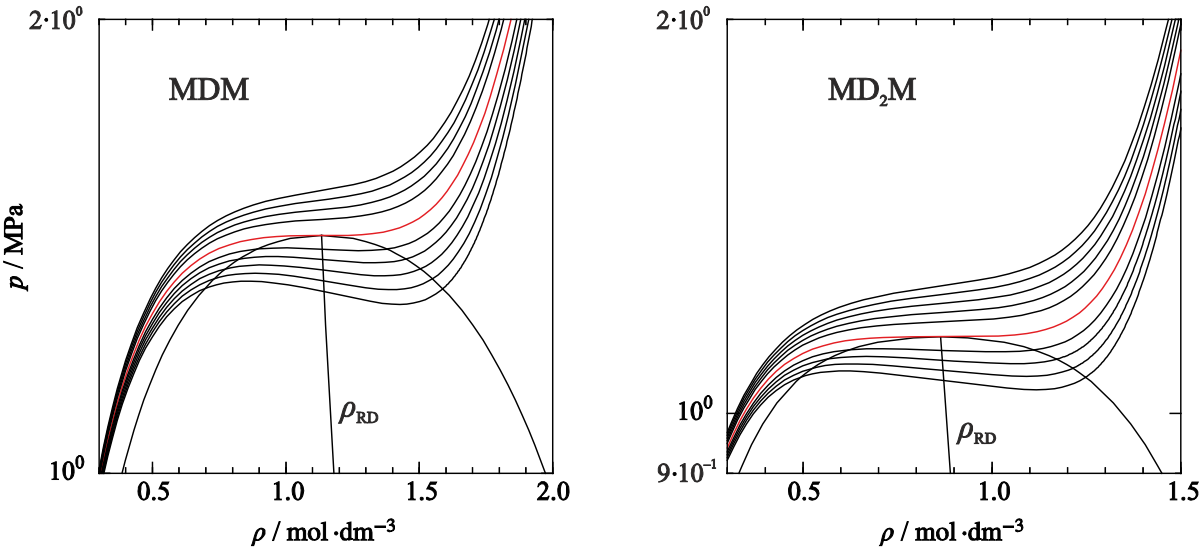

Figure 9. Pressure as function of density along selected isotherms. The critical isotherm is marked in red. Note that the y-axis is presented on a logarithmic scale.

In this way, the critical temperature and density calculated from the equation of state differ from the values given in Table 8 by less than 0.001 %.

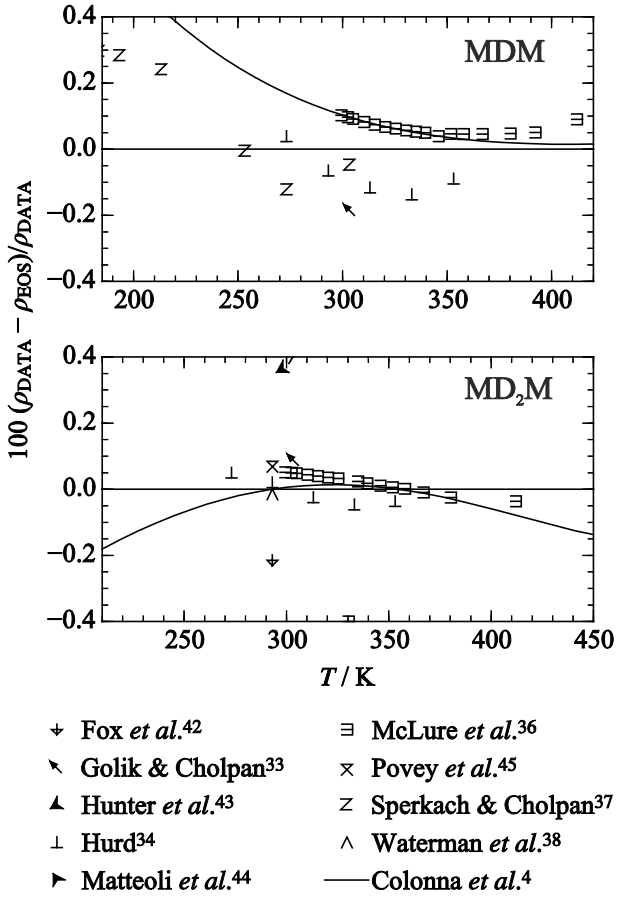

Figure 10. Relative deviations of the homogeneous density data at atmospheric pressure for octamethyltrisiloxane (MDM) and decamethyltetrasiloxane (MD_2M) from the present equations of state.

Relative deviations of experimental density data at atmospheric pressure from the equation of state are depicted in Figure 10. For octamethyltrisiloxane, the equation of Colonna *et al.*[4] agrees better with the course of the data of McLure *et al.*[36] than the present equation of state, and deviations between both equations increase for decreasing temperatures. During the development of the equation in this work, it was not possible to fit to these data more accurately without deteriorating the representation of the homogeneous density data of Abbas *et al.*[9] For decamethyltetrasiloxane, the representation of the data is similar with both equations. The data of McLure *et al.*[36] and Hurd [34] agree much better with each other than in case of octamethyltrisiloxane. This might be an indication that the data of decamethyltetrasiloxane are more accurate than for octamethyltrisiloxane. This assumption is also supported by the representation of the data with the present equations of state. However, for both fluids, deviations do not exceed 0.14 %. Moreover, since Abbas *et al.*[9] measured down to p_{min} = 0.77 MPa, the uncertainty statement of 0.15 % is also assumed to be valid for atmospheric pressure.

Finally, there are some density measurements in the homogeneous gas state for octamethyltrisiloxane available. Figure 7 shows that these data scatter around the present equation of state within approximately 1.5 %. The uncertainty of the data was analyzed in detail for hexamethyldisiloxane by Thol *et al.*[1] and was assessed to be at least 1 %. Except for the highest isotherm (T = 573 K), the data are represented within this uncertainty.

Since the data were measured at very low density, it is possible to extrapolate the isotherms down to vanishing pressure to determine the second thermal virial coefficient B. According to the virial expansion, the compressibility factor can be expressed as

$$Z = \frac{p}{\rho RT} = 1 + B\rho(T) + C\rho^2(T) + \ldots . \qquad (14)$$

Based on this approach, the second virial coefficient can be extrapolated as shown in Figure 11. This figure depicts that the isotherms are self-consistent for $\rho > 0.04$ mol·dm^{-3} only. The low-density data should thus not be considered in such a procedure. Nevertheless, it is not completely clear how the second virial coefficient data of Marcos *et al.*[35] were determined. Especially for 548 K and 573 K, a significant offset persists between the extension of the experimental data and the provided virial coefficients.[35] In spite of this discrepancy, the present equation of state matches with the virial coefficient data better than with the density data. Therefore, the deviations of up to 1.5 % for the low-density data were accepted, whereas the second virial coefficient data are represented within 70 cm^3·mol^{-1} (3 %).

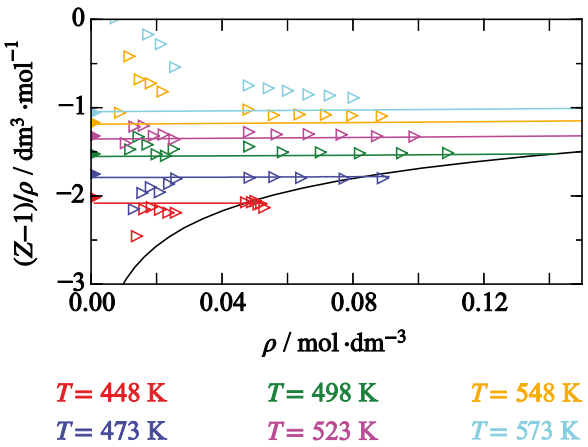

Figure 11. $(Z\text{-}1)/\rho$ as a function of density along six isotherms. Open triangles represent experimental density data of Marcos *et al.*[35], solid triangles mark the extrapolated second thermal virial coefficient data of Marcos *et al.*[35], and the solid lines depict the present equation of state for octamethyltrisiloxane (MDM).

4.3 Caloric properties

In Figures 12 and 13, relative deviations of the speed of sound data measured in this work from the present equations of state are shown. In combination with the density data of Abbas *et al.*,[9] these data formed the basis for the development of the present equations of state. For octamethyltrisiloxane, a temperature range from 300 K to 550 K with a maximum pressure of p = 30 MPa was covered. The data are reproduced within 0.3 %, which is well within the

uncertainty of the data. The equation of Colonna *et al.*[4] deviates by more than 15 % because no density or speed of sound data at elevated pressures were available when the equation was developed. Only three data points of Waterman *et al.*[38] and Weissler[39] at atmospheric pressure were available. However, they were still missed by about 10 % because they were not included in the fitting procedure.[4] With the present equation of state they are reproduced within 3 %, whereby the two data points of Weissler[39] agree well with the data measured in this work. Moreover, they are supported by the data point of Golik and Cholpan.[33] Measurements of Sperkach and Cholpan[37] show positive deviations up to 3 %, whereas the data point of Waterman *et al.*[38] deviates by −2.6 %. For both data sets, no information on the uncertainty is available so that the main focus was given to the correct description of the data measured in this work.

As explained in section 2, another pressure sensor enabled for the measurement of data at higher pressures for the measurements of decamethyltetrasiloxane. Here, a temperature range of 218 K to 500 K with a maximum pressure of p_{max} = 120 MPa was considered. These data are represented within 0.2 %. Considering the accuracy of the apparatus and the sample purity, this is most likely within the measurement uncertainties. For the same reason as in case of octamethyltrisiloxane, the equation of Colonna *et al.*[4] again exhibits large deviations by up to 16 %. The available data of Waterman *et al.*[38] and Weissler[39] were not considered by Colonna *et al.*[4] so that deviations of up to 14.5 % can be observed. These deviations were reduced to approximately 0.5 % in the present work.

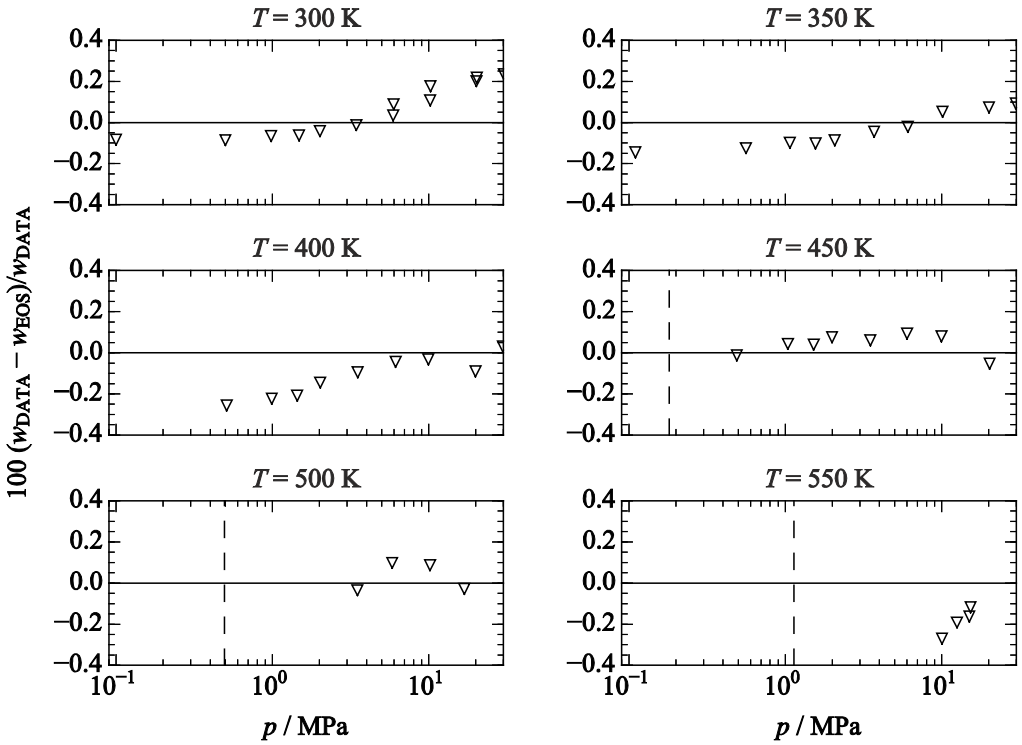

Figure 12. Relative deviations of experimental speed of sound data measured in this work from the present equation of state for octamethyltrisiloxane (MDM).

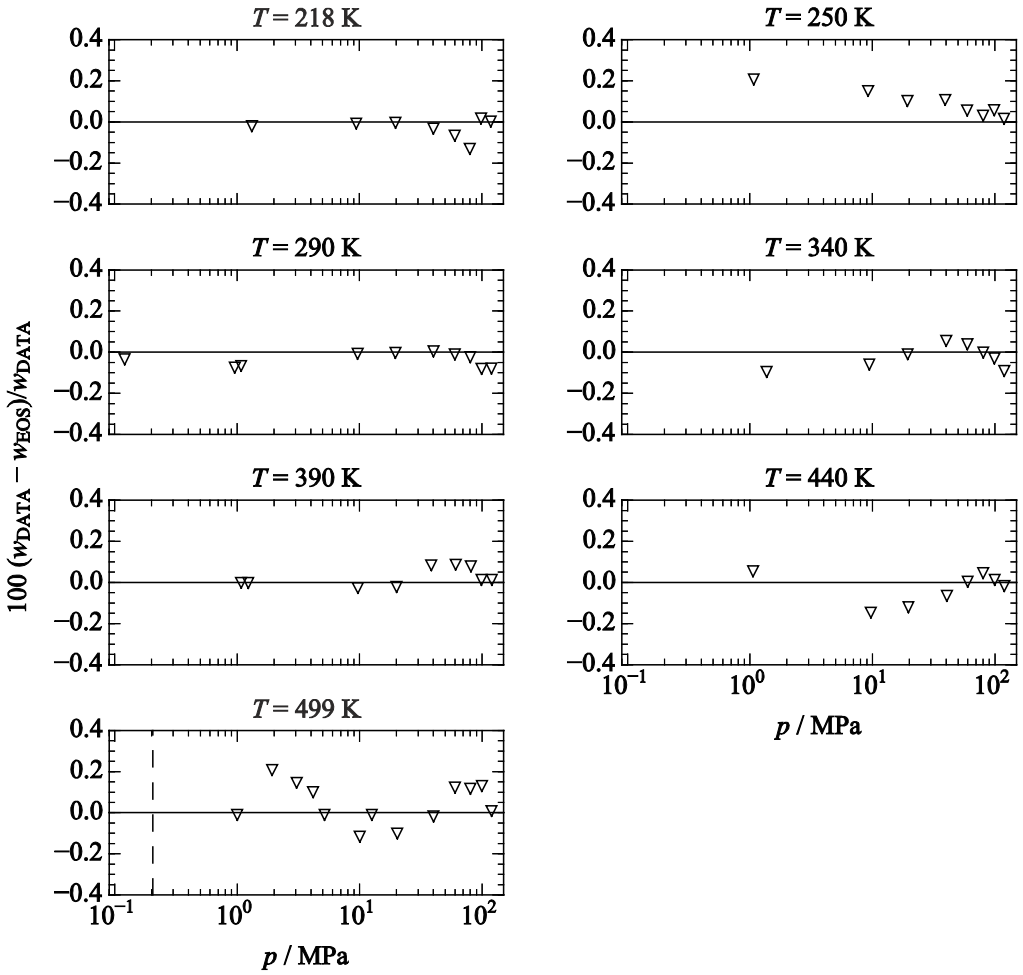

Figure 13. Relative deviations of experimental speed of sound data measured in this work from the present equation of state for decamethyltetrasiloxane (MD_2M).

Figure 14 shows isobaric heat capacity data along the saturated liquid line for both fluids. The experimental uncertainties of the data of Abbas *et al.*[9] are 1 % according to the authors. Therefore, deviations of 0.6 % with respect to the present equations of state are well within these uncertainties. The equations of Colonna *et al.*[4] deviate by up to 5 %. The main reason can be attributed to the inappropriate description of the ideal gas contribution and the speed of sound. A better description of both properties entailed a much better characterization of the isobaric heat capacity.

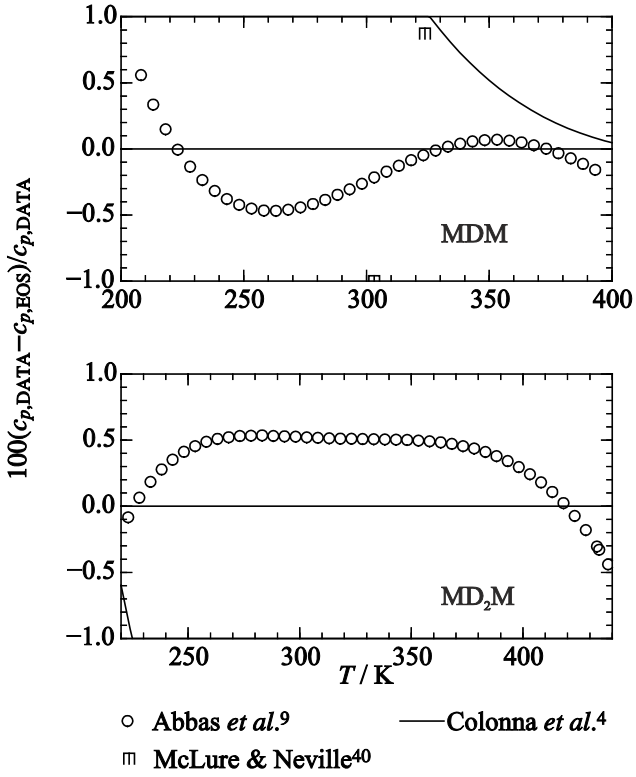

Figure 14. Relative deviations of experimental isobaric heat capacity data of octamethyltrisiloxane (MDM) and decamethyltetrasiloxane (MD_2M) from the present equations of state. Deviations from the equation of Colonna *et al.*[4] is out of range for almost all calculated states for MD_2M.

5 PHYSICAL AND EXTRAPOLATION BEHAVIOR

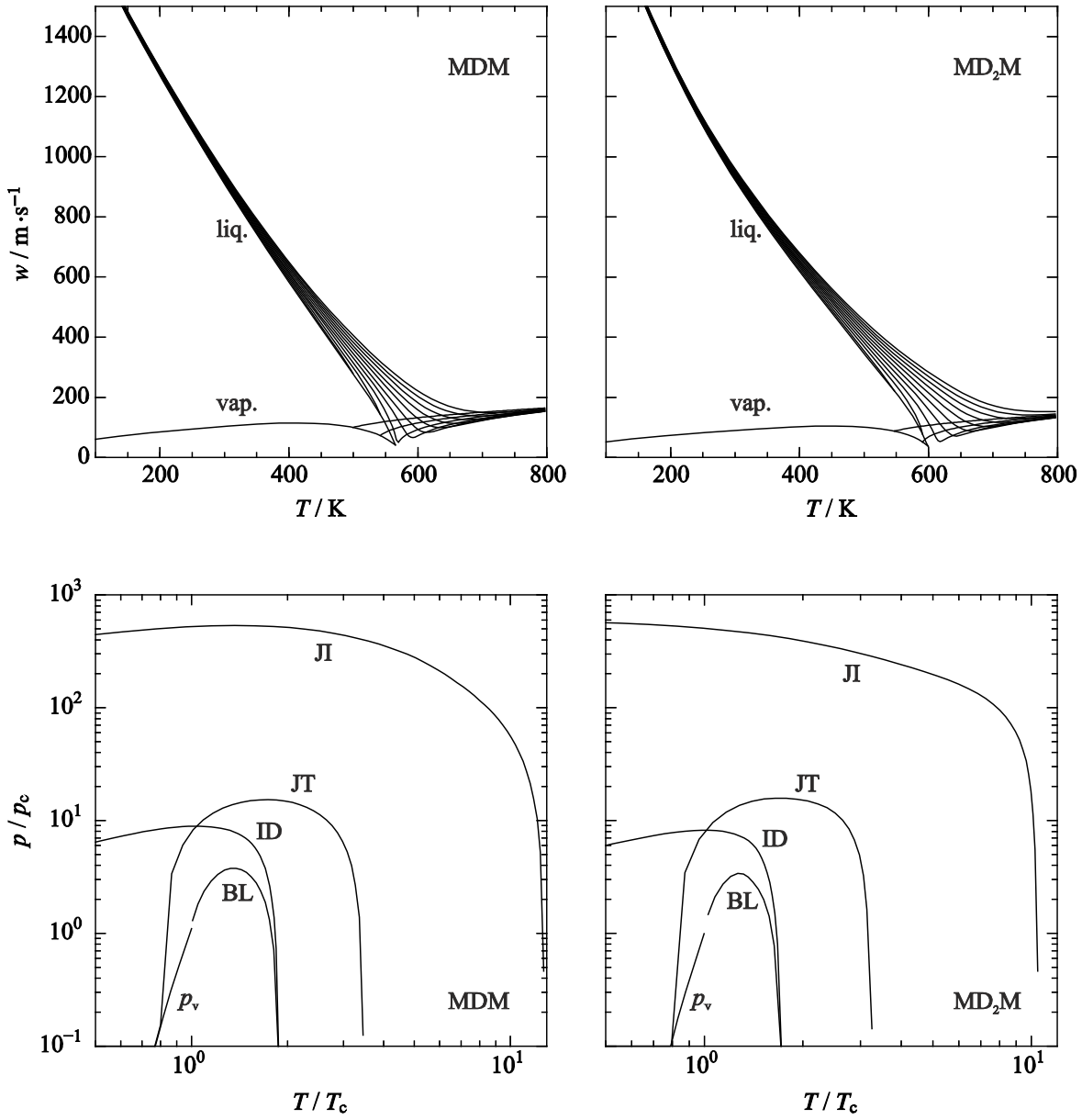

Figure 15. Speed of sound as function of temperature (top) and characteristic ideal curves[54] (bottom) of octamethyltrisiloxane (MDM) and decamethyltetrasiloxane (MD_2M). ID: ideal curve, BL: Boyle curve, JT: Joule-Thomson inversion curve, JI: Joule inversion curve.

The correct description of the physical and extrapolation behavior is a crucial task during the development of equations of state. Many applications require the knowledge of thermodynamic properties not only outside the range of validity (e.g., in mixture models) but also of thermodynamic properties that were not investigated experimentally. Since all thermodynamic properties can be calculated from combinations of the Helmholtz energy and its derivatives with respect to the natural variables, it is possible to predict properties at least qualitatively. Therefore, appropriate behavior was a major aspect in this work. The equation was carefully analyzed by means of characteristic properties, which are well known to be an indication for good extrapolation behavior. Detailed information can be found in the

literature.[20,22,54,55] This includes the isobaric and isochoric heat capacity, speed of sound, phase identification parameter,[56] Grüneisen parameter,[57] characteristic ideal curves,[54] thermal virial coefficients, the thermal behavior ($p\rho T$) at extreme conditions, etc. All of these properties exhibit reasonable behavior, which is representatively shown for the speed of sound and the characteristic ideal curves in Figure 15.

6 BETHE-ZEL'DOVICH-THOMPSON FLUIDS

Because of their special characteristics, siloxanes are considered as working fluids for ORC processes. In this context, the possible affiliation of siloxanes to the class of so-called Bethe-Zel'dovich-Thompson (BZT) fluids is discussed in the literature.[10] This phenomenon is based on theoretical observations of Bethe[58] and Zel'dovich[59] in the 1940s and was applied to ORC working fluids by Thompson[60] in 1971. In ORC processes, turbines are often operated at transonic conditions. This causes huge losses due to distinct pressure gradients evoked by compression waves and the available energy cannot fully be exploited.[61] The basic idea of BZT fluids is that these losses can be reduced with the use of working fluids with unusual behavior in the gaseous regime near the critical point. Numerous studies were conducted to identify such fluids in the literature.[61–64] The decisive criterion for the unusual behavior is the fundamental derivative of gas dynamics introduced by Hayes[65]

$$\Gamma_{\mathrm{GD}} = 1 + \frac{\rho}{w}\left(\frac{\partial w}{\partial \rho}\right)_s = \frac{v^3}{2w^2 M}\left(\frac{\partial^2 p}{\partial v^2}\right)_s . \tag{15}$$

If a fluid exhibits a negative fundamental derivative of gas dynamics along the saturated vapor line, it is considered to be a BZT fluid, which is desired for a particularly effective operation of ORC processes.

Based on their equations of state, Colonna *et al.*[10] suggested siloxanes as possible BZT fluid candidates. However, Eq. (15) shows that this property is highly dependent on the correct description of density and speed of sound. As shown by Thol *et al.*,[1,2] Colonna *et al.*,[3,4] and in this work, the experimental databases were very limited when Colonna *et al.*[3,4] developed their equations of state. With the recent accurate and comprehensive density and speed of sound measurements, the description of these properties by means of the recent equations of state is much more reliable. Thus, the question whether the siloxanes may be BZT fluids is reinvestigated here. Figure 16 shows that the first three linear siloxanes (MM, MDM, MD_2M) and the first cyclic siloxane (D_4) do *not* exhibit a negative fundamental derivative of gas dynamics. The equations of Colonna *et al.*[3,4] already showed this behavior, which is confirmed by the equations presented in Thol *et al.*[1,2] and in this work. In Figure 17, the same property is depicted for four siloxanes of higher order (MD_3M, MD_4M, D_5, and D_6). Except for D_5, according to the equations of Colonna *et al.*,[3,4] all of them *do* show a negative fundamental derivative of gas dynamics, which may lead to the conclusion that those are BZT fluids. However, the underlying equations of state are based on such a weak experimental database that new measurements and equations of state are required for a reliable statement. This task is planned for future work.

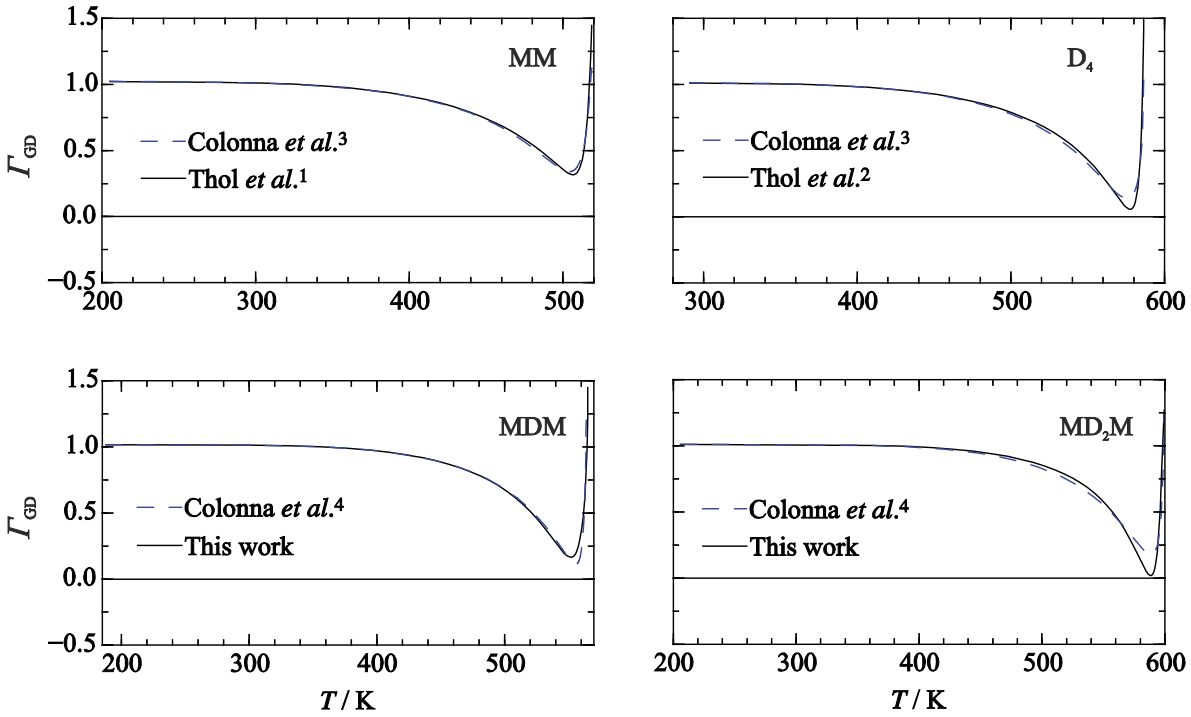

Figure 16. Fundamental derivative of gas dynamics as a function of temperature along the saturated vapor line for MM, MDM, D_4, and MD_2M.

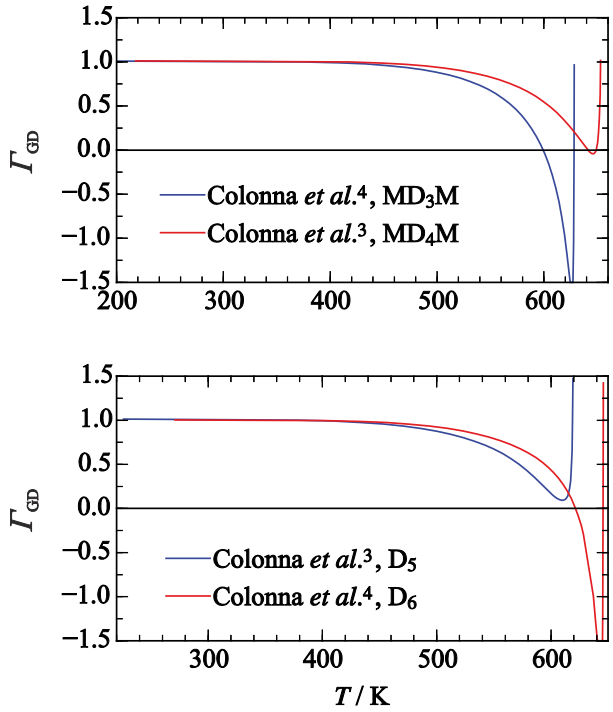

Figure 17. Fundamental derivative of gas dynamics as a function of temperature along the saturated vapor line for MD_3M, MD_4M, D_5, and D_6.

7 CONCLUSION

Equations of state for octamethyltrisiloxane and decamethyltetrasiloxane are presented. Because the experimental database was rather limited, speed of sound measurements were carried out in the compressed liquid as well as in the supercritical region by means of the pulse-echo technique.

The equations are expressed in terms of the Helmholtz energy and can be used to calculate all thermodynamic properties. For both fluids, the ideal contribution contains three Planck-Einstein terms, whereas the residual contribution comprises five polynomial, five exponential, and five Gaussian bell-shaped terms. They are valid from the triple point temperature up to a maximum temperature of $T_{max,MDM}$ = 570 K and $T_{max,MD2M}$ = 600 K with a maximum pressure of p_{max} = 130 MPa. Based on recent density and speed of sound measurements, the representation of these properties could significantly be improved when comparing to the equations of Colonna *et al.*[4] The uncertainty of density data calculated with the new equations of state is expected to be 0.15 %. The speed of sound can be reproduced with an uncertainty of 0.3 % (MDM) and 0.2 % (MD_2M). Calculated vapor pressure data are expected to be accurate to within 0.5 %.

Reference values to verify computer implementation are given in the Appendix. Furthermore, parameter files for the application in the software packages TREND[66] and REFPROP[67] are provided in the supplementary material.

Since siloxanes are considered for the application in ORC processes, the affiliation of these fluids to the so-called Bethe-Zel'dovich-Thompson (BZT) class was analyzed. The results show that MM, MDM, MD_2M, and D_4 exhibit a positive fundamental derivative of gas dynamics along the entire saturated vapor line. Therefore, they are not categorized as BZT fluids.

ACKNOWLEDGEMENT

We thank M. Körber and G. T. Toris for their assistance during the development of the equations of state.

APPENDIX

Table 13. Test values for computer implementation.

T / K	ρ / mol·dm^{-3}	p / MPa	c_p / J·mol^{-1}·K^{-1}	w / m·s^{-1}	h / J·mol^{-1}	s / J·mol^{-1}·K^{-1}	a / J·mol^{-1}
Octamethyltrisiloxane (MDM)							
320	0.0001	$2.659237\cdot10^{-4}$	$3.434178\cdot10^{+2}$	$1.073143\cdot10^{+2}$	$-2.908074\cdot10^{+3}$	$2.842609\cdot10^{+1}$	$-1.466366\cdot10^{+4}$
320	3.5	$2.548165\cdot10^{+1}$	$4.276187\cdot10^{+2}$	$1.025009\cdot10^{+3}$	$-4.446580\cdot10^{+4}$	$-1.407280\cdot10^{+2}$	$-6.713301\cdot10^{+3}$
500	0.05	$1.919677\cdot10^{-1}$	$4.641575\cdot10^{+2}$	$1.237605\cdot10^{+2}$	$6.824950\cdot10^{+4}$	$1.494223\cdot10^{+2}$	$-1.030103\cdot10^{+4}$
500	3	$3.498485\cdot10^{+1}$	$5.164433\cdot10^{+2}$	$7.526067\cdot10^{+2}$	$4.256670\cdot10^{+4}$	$6.633294\cdot10^{+1}$	$-2.261391\cdot10^{+3}$
575	2	$3.511622\cdot10^{+0}$	$5.972631\cdot10^{+2}$	$2.044220\cdot10^{+2}$	$8.116803\cdot10^{+4}$	$1.600291\cdot10^{+2}$	$-1.260453\cdot10^{+4}$
Decamethyltetrasiloxane (MD_2M)							
350	0.0001	$2.908572\cdot10^{-4}$	$4.676281\cdot10^{+2}$	$9.760521\cdot10^{+1}$	$-1.931507\cdot10^{+4}$	$-1.227574\cdot10^{+1}$	$-1.792715\cdot10^{+4}$
350	2.9	$9.764338\cdot10^{+1}$	$5.681542\cdot10^{+2}$	$1.295433\cdot10^{+3}$	$-4.764493\cdot10^{+4}$	$-2.080510\cdot10^{+2}$	$-8.497211\cdot10^{+3}$
500	0.05	$1.848863\cdot10^{-1}$	$5.872108\cdot10^{+2}$	$1.034085\cdot10^{+2}$	$5.810375\cdot10^{+4}$	$1.184514\cdot10^{+2}$	$-4.819665\cdot10^{+3}$
500	2.7	$1.157619\cdot10^{+2}$	$6.494756\cdot10^{+2}$	$1.168896\cdot10^{+3}$	$4.895828\cdot10^{+4}$	$5.385695\cdot10^{+0}$	$3.390654\cdot10^{+3}$
590	2.5	$8.978835\cdot10^{+1}$	$6.856283\cdot10^{+2}$	$9.877431\cdot10^{+2}$	$1.019224\cdot10^{+5}$	$1.210574\cdot10^{+2}$	$-5.416819\cdot10^{+3}$

Supporting Information Available:

Two text files containing the parameters of the equations are available. For the use in TREND[66] or REFPROP[67], they have to be renamed into MDM.FLD and MD2M.FLD.

8 REFERENCES

(1) Thol, M.; Dubberke, F. H.; Rutkai, G.; Windmann, T.; Köster, A.; Span, R.; Vrabec, J., Fundamental Equation of State Correlation for Hexamethyldisiloxane Based on Experimental and Molecular Simulation Data. *Fluid Phase Equilib.* **2016**, *418*, 133–151.

(2) Thol, M.; Rutkai, G.; Köster, A.; Dubberke, F. H.; Windmann, T.; Span, R.; Vrabec, J., Thermodynamic Properties for Octamethylcyclotetrasiloxane. *J. Chem. Eng. Data* **2016**, *61*, 2580–2595.

(3) Colonna, P.; Nannan, N. R.; Guardone, A.; Lemmon, E. W., Multiparameter Equations of State for Selected Siloxanes. *Fluid Phase Equilib.* **2006**, *244*, 193–211.

(4) Colonna, P.; Nannan, N. R.; Guardone, A., Multiparameter Equations of State for Siloxanes: $[(CH_3)_3\text{-Si-}O_{1/2}]_2\text{-}[O\text{-Si-}(CH_3)_2]_{i=1,\ldots,3}$, and $[O\text{-Si-}(CH3)_2]_6$. *Fluid Phase Equilib.* **2008**, *263*, 115–130.

(5) Preißinger, M.; Brüggemann, D., Thermal Stability of Hexamethyldisiloxane (MM) for High-Temperature Organic Rankine Cycle (ORC). *Energies* **2016**, *9*, 183.

(6) Nannan, N. R.; Colonna, P.; Tracy, C. M.; Rowley, R. L.; Hurly, J. J., Ideal-Gas Heat Capacities of Dimethylsiloxanes from Speed-of-Sound Measurements and ab initio Calculations. *Fluid Phase Equilib.* **2007**, *257*, 102–113.

(7) Span, R.; Wagner, W., Equations of State for Technical Applications. I. Simultaneously Optimized Functional Forms for Nonpolar and Polar Fluids. *Int. J. Thermophys.* **2003**, *24*, 1–39.

(8) Span, R.; Wagner, W., Equations of State for Technical Applications. II. Results for Nonpolar Fluids. *Int. J. Thermophys.* **2003**, *24*, 41–109.

(9) Abbas, R.; Schedemann, A.; Ihmels, C. E.; Enders, S.; Gmehling, J., Measurement of Thermophysical Pure Component Properties for a Few Siloxanes Used as Working Fluids for Organic Rankine Cycles. *Ind. Eng. Chem. Res.* **2011**, *50*, 9748–9757.

(10) Colonna, P.; Guardone, A.; Nannan, N. R., Siloxanes: A New Class of Candidate Bethe-Zel'dovich-Thompson Fluids. *Phys. Fluids* **2007**, *19*, 086102.

(11) Dubberke, F. H.; Rasche, D. B.; Baumhögger, E.; Vrabec, J., Apparatus for the Measurement of the Speed of Sound of Ammonia up to High Temperatures and Pressures. *Rev. Sci. Instrum.* **2014**, *85*, 084901.

(12) Meier, K., The Pulse-echo Method for High Precision Measurements of the Speed of Sound in Fluids. Habilitation thesis, University of the Federal Armed Forces, Hamburg (Germany), 2006.

(13) Ball, S. J.; Trusler, J. P. M., Speed of Sound of n-Hexane and n-Hexadecane at Temperatures between 298 and 373 K and Pressures up to 100 MPa. *Int. J. Thermophys.* **2001**, *22*, 427–443.

(14) Benedetto, G.; Gavioso, R. M.; Albo, P. A. G.; Lago, S.; Ripa, D. M.; Spagnolo, R., A Microwave–Ultrasonic Cell for Sound-Speed Measurements in Liquids. *Int. J. Thermophys.* **2005**, *26*, 1651–1665.

(15) Dubberke, F. H.; Baumhögger, E.; Vrabec, J., Burst Design and Signal Processing for the Speed of Sound Measurement of Fluids with the Pulse-echo Technique. *Rev. Sci. Instrum.* **2015**, *86*, 054903.

(16) Mohr, P. J.; Newell, D. B.; Taylor, B. N., CODATA Recommended Values of the Fundamental Physical Constants: 2014. *J. Phys. Chem. Ref. Data* **2016**, *45*, 043102.

(17) Span, R. *Multiparameter Equations of State: An Accurate Source of Thermodynamic Property Data*; Springer: Berlin, 2000.

(18) Setzmann, U.; Wagner, W., A New Equation of State and Tables of Thermodynamic Properties for Methane Covering the Range from the Melting Line to 625 K at Pressures up to 100 MPa. *J. Phys. Chem. Ref. Data* **1991**, *20*, 1061–1155.

(19) Lemmon, Eric W. *Numerical Fitting Algorithm for the Development of Equations of State*, personal communication, 2016.

(20) Lemmon, E. W.; Jacobsen, R. T., A New Functional Form and New Fitting Techniques for Equations of State with Application to Pentafluoroethane (HFC-125). *J. Phys. Chem. Ref. Data* **2005**, *34*, 69–108.

(21) Herrig, S.; Thol, M.; Span, R., A Fundamental Equation of State for Chlorine. *to be submitted,* **2017**.

(22) Lemmon, E. W.; McLinden, M. O.; Wagner, W., Thermodynamic Properties of Propane. III. A Reference Equation of State for Temperatures from the Melting Line to 650 K and Pressures up to 1000 MPa. *J. Chem. Eng. Data* **2009**, *54*, 3141–3180.

(23) Rowley, R. L.; Wilding, W. V.; Oscarson, J.; Yang, Y.; Zuendel, N.; Daubert, T.; Danner, R. *DIPPR Data Compilation of Pure Chemical Properties*; Taylor & Francis Publishing Company: New York, 2004.

(24) Dickinson, E.; McLure, I. A., Thermodynamics of n-Alkane + Dimethylsiloxane Mixtures: Part 1.-Gas-Liquid Critical Temperatures and Pressures. *J. Chem. Soc. Faraday Trans. 1* **1974**, *70*, 2313–2320.

(25) Lindley, D. D.; Hershey, H. C., The Orthobaric Region of Octamethyltrisiloxane. *Fluid Phase Equilib.* **1990**, *55*, 109–124.

(26) Flaningam, O. L., Vapor Pressures of Poly(dimethylsiloxane) Oligomers. *J. Chem. Eng. Data* **1986**, *31*, 266–272.

(27) Wieser, M. E.; Berglund, M., Atomic Weights of the Elements 2007 (IUPAC Technical Report). *Pure Appl. Chem.* **2009**, *81*, 2131–2156.

(28) Patnode, W.; Wilcock, D. F., Methylpolysiloxanes. *J. Am. Chem. Soc.* **1946**, *68*, 358–363.

(29) Reuther, H.; Reichel, G., Über Silikone XXVI: Über den Dampfdruck und die Verdampfungswärme einiger definierter siliziumorganischer Verbindungen. *Chem. Tech.* **1954**, *6*, 479–480.

(30) Thompson, R., 392. Heats of Combustion and Formation of Some Linear Polydimethylsiloxanes; the Si–C and Si–O Bond-Energy Terms. *J. Chem. Soc.* **1953**, 1908–1914.

(31) Wilcock, D. F., Vapor Pressure-Viscosity Relations in Methylpolysiloxanes. *J. Am. Chem. Soc.* **1946**, *68*, 691–696.

(32) Nannan, N. R.; Colonna, P., Improvement on Multiparameter Equations of State for Dimethylsiloxanes by Adopting More Accurate Ideal-Gas Isobaric Heat Capacities: Supplementary to P. Colonna, N.R. Nannan, A. Guardone, E.W. Lemmon, Fluid Phase Equilib. 244, 193 (2006). *Fluid Phase Equilib.* **2009**, *280*, 151–152.

(33) Golik, O. Z.; Cholpan, P. P., Molecular Structure, Compressibility, Surface Tension and Viscosity of Some Polysiloxanes. *Ukr. Fiz. Zh.* **1960**, *5*, 242–251.

(34) Hurd, C. B., Studies on Siloxanes: I. The Specific Volume and Viscosity in Relation to Temperature and Constitution. *J. Am. Chem. Soc.* **1946**, *68*, 364–370.

(35) Marcos, D. H.; Lindley, D. D.; Wilson, K. S.; Kay, W. B.; Hershey, H. C., A (p, V, T) Study of Tetramethylsilane, Hexamethyldisiloxane, Octamethyltrisiloxane, and Toluene from 423 to 573 K in the Vapor Phase. *J. Chem. Thermodyn.* **1983**, *15*, 1003–1014.

(36) McLure, I. A.; Pretty, A. J.; Sadler, P. A., Specific Volumes, Thermal Pressure Coefficients, and Derived Quantities of Five Dimethylsiloxane Oligomers from 25 to 140 °C. *J. Chem. Eng. Data* **1977**, *22*, 372–376.

(37) Sperkach, V.; Choplan, F., Study of Acoustic Scattering in Some Siloxanes. *Fiz. Zhidk. Sostoyaniya* **1979**, 104–109.

(38) Waterman, H. I.; van Herwijnen, W. E. R.; Den Hartog, H. W., Statistical-Graphical Survey of Series of Linear and Cyclic Dimethylsiloxanes. *J. Appl. Chem.* **1958**, *8*, 625–631.

(39) Weissler, A., Ultrasonic Investigation of Molecular Properties of Liquids. III. 1 Linear Polymethylsiloxanes 2. *J. Am. Chem. Soc.* **1949**, *71*, 93–95.

(40) McLure, I. A.; Neville, J. F., An Analysis of the Gas-Liquid Critical Properties of the Dimethylsiloxanes Establishing Tetramethylsilane as the Forerunner of the Series. *J. Chem. Thermodyn.* **1977**, *9*, 957–961.

(41) Wabiszczewicz, M., Vermessung und Auswertung der Verdampfungsenthalpie der Siloxane Decamethylcyclopentasiloxan (D5), Octamethyltrisiloxan (MDM) und Hexamethyldisiloxan (MM) unter Verwendung eines Differenzkalorimeters. Bachelorarbeit, Universität Paderborn, Paderborn, 2014.

(42) Fox, H.; Taylor, P.; Zisman, W., Polyorganosiloxanes…: Surface Active Properties. *Ind. Eng. Chem.* **1947**, *39*, 1401–1409.

(43) Hunter, M. J.; Warrick, E. L.; Hyde, J. F.; Currie, C. C., Organosilicon Polymers: II. The Open Chain Dimethylsiloxanes with Trimethylsiloxy End Groups. *J. Am. Chem. Soc.* **1946**, *68*, 2284–2290.

(44) Matteoli, E.; Gianni, P.; Lepori, L.; Spanedda, A., Thermodynamic Study of Heptane + Silicone Mixtures. Excess Volumes and Enthalpies at 298.15 K. *J. Chem. Eng. Data* **2011**, *56*, 5019–5027.

(45) Povey, M. J. W.; Hindle, S. A.; Kennedy, J. D.; Stec, Z.; Taylor, R. G., The Molecular Basis for Sound Velocity in n-Alkanes, 1-Alcohols and Dimethylsiloxanes. *Phys. Chem. Chem. Phys.* **2003**, *5*, 73–78.

(46) Scott, D. W.; Messerly, J. F.; Todd, S. S.; Guthrie, G. B.; Hossenlopp, I. A.; Moore, R. T.; Osborn, A.; Berg, W. T.; McCullough, J. P., Hexamethyldisiloxane: Chemical Thermodynamic Properties and Internal Rotation about the Siloxane Linkage. *J. Phys. Chem.* **1961**, *65*, 1320–1326.

(47) Mosin, A. M.; Mikhailov, A. M., Thermodynamic Functions of Hexamethyldisiloxane. *Zh. Fiz. Khim.* **1972**, *46*, 537.

(48) Kay, W. B., The Vapor Pressures and Saturated Liquid and Vapor Densities of the Isomeric Hexane. *J. Am. Chem. Soc.* **1946**, *68*, 1336–1339.

(49) Kay, W. B.; Donham, W. E., Liquid-Vapor Equilibria in the Iso-Butanol-n-Butanol, Methanol-n-Butanol and Diethylether-n-Butanol Systems. *Chem. Eng. Sci.* **1955**, *4*, 1–16.

(50) Wagner, W.; Pruss, A., The IAPWS Formulation 1995 for the Thermodynamic Properties of Ordinary Water Substance for General and Scientific Use. *J. Phys. Chem. Ref. Data* **2002**, *31*, 387–535.

(51) Lemmon, E. W.; Span, R., Short Fundamental Equations of State for 20 Industrial Fluids. *J. Chem. Eng. Data* **2006**, *51*, 785–850.

(52) Abbas, R., Anwendung der Gruppenbeitragszustandsgleichung VTPR für die Analyse von reinen Stoffen und Mischungen als Arbeitsmittel in technischen Kreisprozessen. Ph.D. thesis, Technische Universität Berlin, Berlin, 2011.

(53) Schedemann, A., Aufbau und Inbetriebnahme einer Dichtemessanlage. Messung und Modellierung des PVT-Verhaltens bis zu Drücken von 1400 bar. Diploma thesis, Universität Oldenburg, Oldenburg, 2009.

(54) Span, R.; Wagner, W., On the Extrapolation Behavior of Empirical Equations of State. *Int. J. Thermophys.* **1997**, *18*, 1415–1443.

(55) Thol, M.; Rutkai, G.; Köster, A.; Span, R.; Vrabec, J.; Lustig, R., Equation of State for the Lennard-Jones Fluid. *J. Phys. Chem. Ref. Data* **2016**, *45*, 023101.

(56) Venkatarathnam, G.; Oellrich, L. R., Identification of the Phase of a Fluid Using Partial Derivatives of Pressure, Volume, and Temperature without Reference to Saturation Properties: Applications in Phase Equilibria Calculations. *Fluid Phase Equilib.* **2011**, *301*, 225–233.

(57) Arp, V.; Persichetti, J. M.; Chen, G.-b., The Grüneisen Parameter in Fluids. *J. Fluids Eng.* **1984**, *106*, 193–201.

(58) Bethe, H. A., On the Theory of Shock Waves for an Arbitrary Equation of State. In *Classic Papers in Shock Compression Science*; Johnson, J. N., Chéret, R., Eds.; High-Pressure Shock Compression of Condensed Matter; Springer: New York, NY, 1998; pp 421–495.

(59) Zel'dovich, Y. B. *Theory of Shock Waves and Introduction to Gas Dynamics*; Izdatel'stvo Akademii Nauk SSSR: Moscow, 1946.

(60) Thompson, P. A., A Fundamental Derivative in Gasdynamics. *Phys. Fluids* **1971**, *14*, 1843–1849.

(61) Brown, B. P.; Argrow, B. M., Application of Bethe-Zel'dovich-Thompson Fluids in Organic Rankine Cycle Engines. *J. Propul. Power* **2000**, *16*, 1118–1124.

(62) Schnerr, G. H.; Leidner, P., Diabatic Supersonic Flows of Dense Gases. *Phys. Fluids A* **1991**, *3*, 2445–2458.

(63) Cramer, M. S., Nonclassical Dynamics of Classical Gases. In *Nonlinear Waves in Real Fluids*; Kluwick, A., Ed.; Springer Vienna: Vienna, 1991.

(64) Fergason, S.; Guardone, A.; Argrow, B., Construction and Validation of a Dense Gas Shock Tube. *J. Thermophys. Heat Transfer* **2003**, *17*, 326–333.

(65) Hayes, W. D., The Basic Theory of Gasdynamic Discontinuities. In *Fundamentals of Gas Dynamics. High Speed Aerodynamics and Jet Propulsion, Vol. III*, 1st ed.; Emmons, H. W., Ed.; Princeton University Press: Princeton, 1958.

(66) Span, R.; Eckermann, T.; Herrig, S.; Hielscher, S.; Jäger, A.; Thol, M. *TREND. Thermodynamic Reference and Engineering Data 3.0*; Lehrstuhl für Thermodynamik, Ruhr-Universität Bochum: Bochum, Germany, 2016.

(67) Lemmon, E. W.; Bell, I. H.; Huber, M. L.; McLinden, M. O. *NIST Standard Reference Database 23: Reference Fluid Thermodynamic and Transport Properties-REFPROP, Version 9.1.1*; National Institute of Standards and Technology: Gaithersburg, USA, 2014.